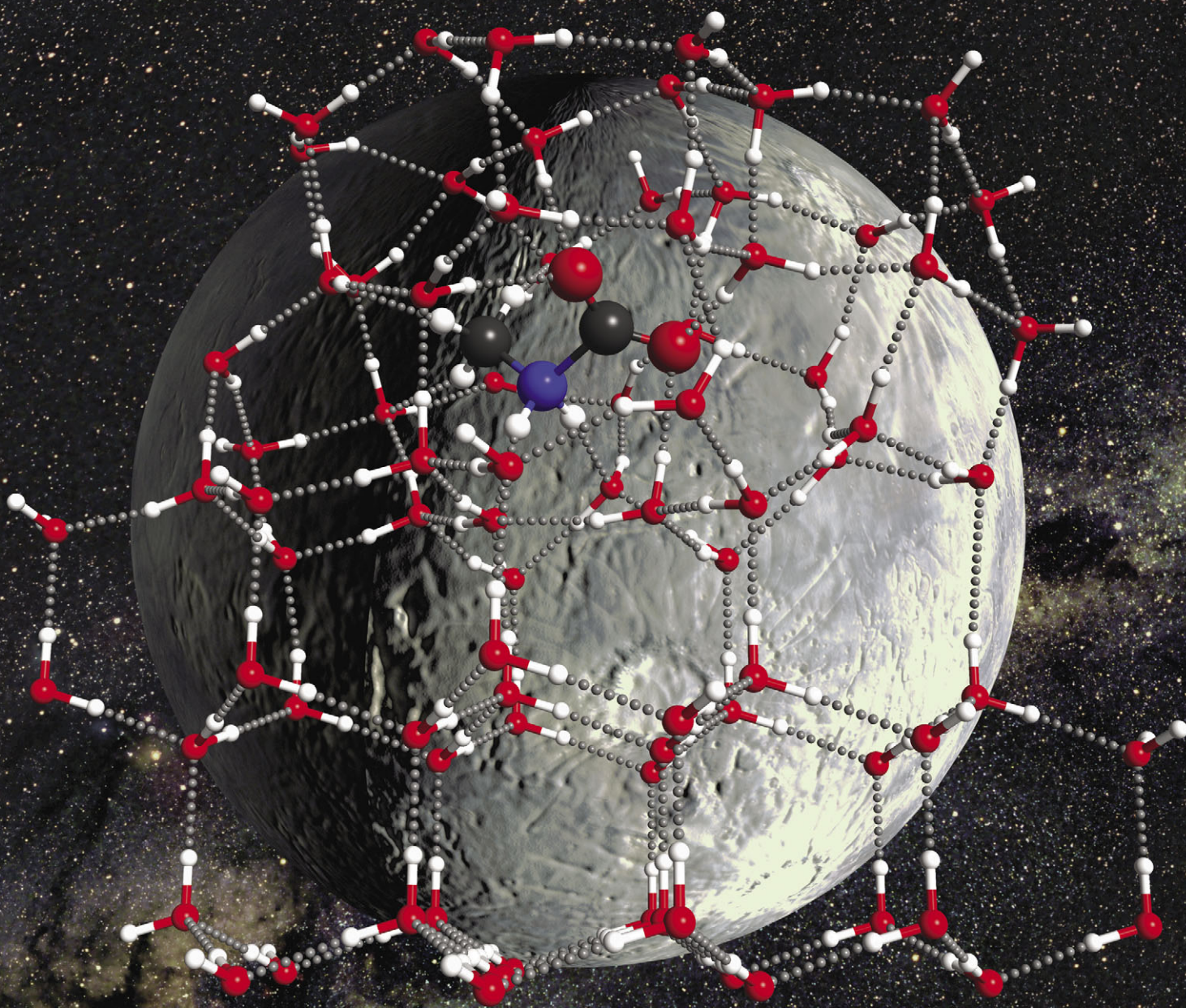


# PCCP

Physical Chemistry Chemical Physics

[www.rsc.org/pccp](http://www.rsc.org/pccp)

Volume 13 | Number 23 | 21 June 2011 | Pages 10825–11452



ISSN 1463-9076

**COVER ARTICLE**

Head *et al.*  
A computational study on  
the structures of methylamine–  
carbon dioxide–water clusters

**HOT ARTICLE**

Donahue *et al.*  
Adventures in ozoneland:  
down the rabbit-hole



1463-9076(2011)13:23;1-X

Cite this: *Phys. Chem. Chem. Phys.*, 2011, **13**, 11083–11098

www.rsc.org/pccp

PAPER

# A computational study on the structures of methylamine–carbon dioxide–water clusters: evidence for the barrier free formation of the methylcarbamic acid zwitterion ( $\text{CH}_3\text{NH}_2^+ \text{COO}^-$ ) in interstellar water ices

Hakan Kayi,<sup>a</sup> Ralf I. Kaiser<sup>ab</sup> and John D. Head<sup>\*a</sup>

Received 28th September 2010, Accepted 18th January 2011

DOI: 10.1039/c0cp01962c

We investigated theoretically the interaction between methylamine ( $\text{CH}_3\text{NH}_2$ ) and carbon dioxide ( $\text{CO}_2$ ) in the presence of water ( $\text{H}_2\text{O}$ ) molecules thus simulating the geometries of various methylamine–carbon dioxide complexes ( $\text{CH}_3\text{NH}_2/\text{CO}_2$ ) relevant to the chemical processing of icy grains in the interstellar medium (ISM). Two approaches were followed. In the amorphous water phase approach, structures of methylamine–carbon dioxide–water [ $\text{CH}_3\text{NH}_2/\text{CO}_2/(\text{H}_2\text{O})_n$ ] clusters ( $n = 0\text{--}20$ ) were studied using density functional theory (DFT). In the crystalline water approach, we simulated methylamine and carbon dioxide interactions on a fragment of the crystalline water ice surface in the presence of additional water molecules in the  $\text{CH}_3\text{NH}_2/\text{CO}_2$  environment using DFT and effective fragment potentials (EFP). Both the geometry optimization and vibrational frequency analysis results obtained from these two approaches suggested that the surrounding water molecules which form hydrogen bonds with the  $\text{CH}_3\text{NH}_2/\text{CO}_2$  complex draw the carbon dioxide closer to the methylamine. This enables, when two or more water molecules are present, an electron transfer from methylamine to carbon dioxide to form the methylcarbamic acid zwitterion,  $\text{CH}_3\text{NH}_2^+ \text{CO}_2^-$ , in which the carbon dioxide is bent. Our calculations show that the zwitterion is formed without involving any electronic excitation on the ground state surface; this structure is only stable in the presence of water, *i.e.* in a methyl amine–carbon dioxide–water ice. Notably, in the vibrational frequency calculations on the methylcarbamic acid zwitterion and two water molecules we find the carbon dioxide asymmetric stretch is *drastically red shifted* by  $435 \text{ cm}^{-1}$  to  $1989 \text{ cm}^{-1}$  and the carbon dioxide symmetric stretch becomes strongly infrared active. We discuss how the methylcarbamic acid zwitterion  $\text{CH}_3\text{NH}_2^+ \text{CO}_2^-$  might be experimentally and astronomically identified by its asymmetric  $\text{CO}_2$  stretching mode using infrared spectroscopy.

## 1. Introduction

Scientists have been enamored by the Interstellar Medium (ISM) for more than half a century, particularly after the detection of astrobiologically important molecules such as the sugar glycolaldehyde ( $\text{HCOCH}_2\text{OH}$ ) toward the hot molecular core Sagittarius B2 (Sgr-B2).<sup>1</sup> In the interstellar medium, dense molecular clouds consist predominantly of gaseous molecules (99%) with molecular hydrogen being dominant and ice-coated grain particles of up to a few 100 nm in diameter at a level of typically 1%.<sup>2–5</sup> Astrochemists have a special interest in the origin and formation of amino acids because their presence in the ISM may provide clues to the delivery of prebiotic molecules

to the early Earth, the origins of life on Earth,<sup>6–8</sup> and the possibility of Earth-like life elsewhere in the universe.<sup>9</sup> Hitherto amino acids were detected in meteorites such as Murchison, Murray, Orgueil and Ivuna;<sup>10–13</sup> up to 80 of them were found in the Murchison meteorite alone.<sup>14,15</sup> In extraterrestrial environments, the simplest amino acid glycine ( $\text{NH}_2\text{CH}_2\text{COOH}$ ) was identified in meteorites like Murchison, Orgueil and Ivuna<sup>12,14</sup> and also in cometary samples returned within the framework of the Stardust mission to comet 81P/Wild 2.<sup>16,17</sup> However, the detection of glycine in the interstellar medium has not been confirmed yet. Although Kuan *et al.* published the first time detection of interstellar glycine,<sup>18</sup> their interpretation was disputed.<sup>19–21</sup>

Due to the importance of glycine ( $\text{NH}_2\text{CH}_2\text{COOH}$ ) as the simplest amino acids and as a building block of polypeptides, several different formation mechanisms have been proposed. Proposals for reactions in the gas-phase include gamma- and

<sup>a</sup> Department of Chemistry, University of Hawaii at Manoa, Honolulu, HI 98622, USA. E-mail: johnh@hawaii.edu

<sup>b</sup> NASA Astrobiology Institute, University of Hawaii at Manoa, Honolulu, HI 96822, USA

X-ray irradiation of carbon-source (carbon monoxide; CO or methane; CH<sub>4</sub>) and nitrogen-source (nitrogen; N<sub>2</sub> or ammonia; NH<sub>3</sub>) gas mixtures<sup>22</sup> and ion–molecule reactions of protonated and ionized hydroxylamine (NH<sub>n</sub>OH<sup>+</sup>; *n* = 2, 3) with formic acid (CH<sub>3</sub>COOH).<sup>23</sup> Several other reactions in the solid-state such as proton irradiation of propane (C<sub>3</sub>H<sub>8</sub>), ammonia (NH<sub>3</sub>), water (H<sub>2</sub>O),<sup>24</sup> UV irradiation of water (H<sub>2</sub>O), methanol (CH<sub>3</sub>OH), ammonia (NH<sub>3</sub>), carbon monoxide (CO), carbon dioxide (CO<sub>2</sub>),<sup>25</sup> UV photolysis of water (H<sub>2</sub>O), methanol (CH<sub>3</sub>OH), ammonia (NH<sub>3</sub>), hydrogen cyanide (HCN),<sup>26</sup> electron irradiation of methylamine (CH<sub>3</sub>NH<sub>2</sub>) and carbon dioxide (CO<sub>2</sub>) ice mixtures,<sup>27</sup> and UV irradiated ice analogs consisting of water (H<sub>2</sub>O), methylamine (CH<sub>3</sub>NH<sub>2</sub>) and carbon dioxide (CO<sub>2</sub>) were also proposed. Holtom *et al.* investigated the formation of glycine (NH<sub>2</sub>CH<sub>2</sub>COOH) and its isomer methylcarbamic acid (CH<sub>3</sub>NHCOOH) *via* secondary electrons generated in the track of galactic cosmic ray particles in extraterrestrial ices.<sup>27</sup> In their experiments, interstellar ice analogs consisting of a methylamine (CH<sub>3</sub>NH<sub>2</sub>) and carbon dioxide (CO<sub>2</sub>) mixture at 10 K were irradiated by 5 keV electrons. Their results indicated the formation of glycine and its methylcarbamic acid isomer at a ratio of about 10 : 1; their findings exposed for the first time detailed reaction mechanisms for glycine and its isomer methylcarbamic acid formation at low temperatures characteristic of interstellar grains in cold molecular clouds such as TMC-1. Further, Lee *et al.* investigated the effect of UV irradiation on interstellar ice-analog films composed of water (H<sub>2</sub>O), methylamine (CH<sub>3</sub>NH<sub>2</sub>) and carbon dioxide (CO<sub>2</sub>).<sup>28</sup> Water dominant samples were exposed to UV light at 56 K. Their results from mass spectroscopic analysis indicated the photochemical synthesis of glycine (NH<sub>2</sub>CH<sub>2</sub>COOH) and its isomers methylcarbamic acid (CH<sub>3</sub>NHCOOH) and methylcarbamate ester (NH<sub>2</sub>COOCH<sub>3</sub>). Recently, Bossa *et al.* investigated the thermal reactivity between methylamine (CH<sub>3</sub>NH<sub>2</sub>) and carbon dioxide (CO<sub>2</sub>) at low temperatures.<sup>29</sup> They detected methylammonium methylcarbamate [CH<sub>3</sub>NH<sub>3</sub><sup>+</sup>][CH<sub>3</sub>NHCO<sub>2</sub><sup>-</sup>] using FTIR spectroscopy. At 248 K from a mass spectrum obtained using a residual gas analyzer they also detected methylcarbamic acid where the most intense peaks in the spectrum were obtained for COO<sup>+</sup> and CH<sub>3</sub>NH<sub>2</sub><sup>+</sup> indicating that gas phase methylcarbamic acid is not stable and decomposes into CH<sub>3</sub>NH<sub>2</sub> and CO<sub>2</sub>. Their detailed data analysis suggested that the formation of the glycine salt, methylammonium glycinate [CH<sub>3</sub>NH<sub>3</sub><sup>+</sup>][NH<sub>2</sub>CH<sub>2</sub>CO<sub>2</sub><sup>-</sup>], is induced by UV irradiation of the methylammonium methylcarbamate [CH<sub>3</sub>NH<sub>3</sub><sup>+</sup>][CH<sub>3</sub>NHCO<sub>2</sub><sup>-</sup>]. In another study, Bossa *et al.* investigated a water-dominated ice<sup>30</sup> consisting of H<sub>2</sub>O : CO<sub>2</sub> : CH<sub>3</sub>NH<sub>2</sub> in the ratio 10 : 3 : 0.5 and again concluded from FTIR spectroscopy that methylammonium methylcarbamate [CH<sub>3</sub>NH<sub>3</sub><sup>+</sup>][CH<sub>3</sub>NHCO<sub>2</sub><sup>-</sup>] is formed which could then be processed by UV radiation to produce the glycine salt. Recently, Goldman *et al.*<sup>31</sup> suggested that impact-induced shock compression of cometary ices followed by expansion to ambient conditions can produce glycine-containing complexes.

Besides the laboratory simulation experiments, the formation of amino acids from simple precursor molecules has also been tackled theoretically. Although numerous computational studies have been conducted on glycine (NH<sub>2</sub>CH<sub>2</sub>COOH)<sup>32–36</sup> including its neutral and zwitterionic forms in aqueous environments,<sup>37–41</sup>

theoretical studies on methylamine (CH<sub>3</sub>NH<sub>2</sub>) and carbon dioxide (CO<sub>2</sub>) interactions are relatively scarce. Andres *et al.* investigated the addition reaction of carbon dioxide to methylamine at the *ab initio* level of theory using different basis sets, and examined the relation between transition state structures and reactivity.<sup>42</sup> In related RHF/3-21G calculations, Jamroz *et al.* investigated the proton transfer from dimethylamine [(CH<sub>3</sub>)<sub>2</sub>NH] to carbon dioxide (CO<sub>2</sub>).<sup>43</sup> They found the lowest barrier to proton transfer from the amino group (NH=) to the carbon dioxide (CO<sub>2</sub>) was obtained when the transition state calculation was started from a 1 : 2 complex containing one carbon dioxide and two dimethylamine [(CH<sub>3</sub>)<sub>2</sub>NH] molecules. The lowest energy equilibrium structure for the 1 : 2 complex is cyclic consisting of the carbon atom from carbon dioxide being drawn towards the nitrogen atom on one of the dimethylamine molecules while the second dimethylamine forms a hydrogen bond bridge between an oxygen atom of carbon dioxide and an amine proton on the first dimethylamine.<sup>43</sup> Holtom *et al.* reported the optimized geometries for the van der Waals complex of methylamine and carbon dioxide (CH<sub>3</sub>NH<sub>2</sub>/CO<sub>2</sub>) and for different conformers of glycine (NH<sub>2</sub>CH<sub>2</sub>COOH).<sup>27</sup> Recently, Bossa *et al.* performed calculations to aid in interpreting their experimentally observed barrier of 4.0 ± 0.2 kJ mol<sup>-1</sup> for the proton transfer from methylamine and carbon dioxide to produce methylcarbamic acid (CH<sub>3</sub>NHCOOH).<sup>29</sup> Just as in the study by Jamroz *et al.*,<sup>43</sup> they also found their calculated barriers to proton transfer were reduced for the (CH<sub>3</sub>NH<sub>2</sub>)<sub>*n*</sub>/CO<sub>2</sub> complexes when *n* was increased from one to three. The extra methylamine (CH<sub>3</sub>NH<sub>2</sub>) provides a cooperative binding effect by forming hydrogen bond bridges between the interacting methylamine and carbon dioxide, where the bridging methylamine could also act as a shuttle for the methylamine proton to carbon dioxide. In both studies, the presence of the additional bridging methylamine (CH<sub>3</sub>NH<sub>2</sub>) or dimethylamine [(CH<sub>3</sub>)<sub>2</sub>NH] molecules not only decreased the proton transfer activation energies, but they also caused significant bending in the carbon dioxide bond angle and a major decrease in the nitrogen–carbon (N–C) distance separating the amine group on the methylamine interacting with the carbon dioxide.<sup>29,43</sup>

The above calculations suggest that any molecule which can form a hydrogen bond bridge between carbon dioxide (CO<sub>2</sub>) and methylamine (CH<sub>3</sub>NH<sub>2</sub>) might draw the two molecules closer together and reduce the barrier for proton transfer between the two molecules. Besides the methylamine–carbon dioxide (CH<sub>3</sub>NH<sub>2</sub>/CO<sub>2</sub>) system, there have been a number of calculations for carbon dioxide in different sized water only clusters and these calculations generally produce optimized structures where the carbon dioxide stays linear except when a proton is transferred to the carbon dioxide. Previously, Khan calculated the bond angle of carbon dioxide in water cluster cages containing 24 and 28 water molecules to be 179° and 178°, respectively, using HF/6-31G(d) calculations.<sup>44</sup> Jena and Mishra calculated the bending of carbon dioxide in a range between 1.5° and 2.9° for carbon dioxide–water clusters [CO<sub>2</sub>(H<sub>2</sub>O)<sub>*n*</sub>; *n* = 1–6] at different levels of theory for the ground state structures.<sup>45</sup> Peterson *et al.* concluded that the carbon dioxide could be bent by about 3–4°, but it is very unlikely that it is bent by more than 5° according to their

experimental microwave spectroscopic findings for the carbon dioxide with a two water  $[\text{CO}_2(\text{H}_2\text{O})_2]$  system.<sup>46</sup>

Due to the importance of the methylamine–carbon dioxide ( $\text{CH}_3\text{NH}_2/\text{CO}_2$ ) system as a potential precursor to glycine and its isomer, we have performed quantum chemistry calculations to simulate the possible interactions taking place between a pair of individual methylamine and carbon dioxide molecules in the presence of a water ice matrix. The waters in these calculations are intended to simulate the dominant water component of interstellar ices in cold molecular clouds. The calculations examine how the methylamine–carbon dioxide structural properties and vibrational frequencies evolve in the presence of an increasing number of water molecules. We utilized two different procedures to incorporate water in the calculations. First, we performed geometry optimizations on several different clusters of the type  $\text{CH}_3\text{NH}_2/\text{CO}_2/(\text{H}_2\text{O})_n$  where  $n$  ranged from 0 to 20 and the water has an amorphous structure. Thereafter, we performed calculations on  $\text{CH}_3\text{NH}_2/\text{CO}_2/(\text{H}_2\text{O})_n$  clusters with  $n$  ranging between 52 and 82 of the water molecules arranged as a fragment of the low temperature crystalline ice XI phase structure which is formed below 72 K. The two approaches are highly complementary. The paper is organized as follows. The next section describes the computational methods used along with details on how the different initial  $\text{CH}_3\text{NH}_2/\text{CO}_2/(\text{H}_2\text{O})_n$  cluster structures were generated. This is followed by the Results and Discussion section where the optimized geometries and computed vibrational frequencies obtained for the amorphous water and crystalline water clusters are presented. Concluding remarks are given in the final section of the paper.

## 2. Computational method

Geometry optimizations were performed first on specific  $\text{CH}_3\text{NH}_2/\text{CO}_2/(\text{H}_2\text{O})_n$  ( $n = 0\text{--}20$ ) to simulate amorphous water clusters. Typically 20 initial structures for most of the smaller clusters were generated by randomly arranging water molecules around an initially guessed  $\text{CH}_3\text{NH}_2/\text{CO}_2$  structure whereas about 10 initial larger cluster geometries were generated by randomly adding extra water to a previously optimized smaller  $\text{CH}_3\text{NH}_2/\text{CO}_2/(\text{H}_2\text{O})_m$  structure with  $m < n$ . While this geometry optimization procedure only samples a small fraction of the possible stable  $\text{CH}_3\text{NH}_2/\text{CO}_2/(\text{H}_2\text{O})_n$  conformations and should not be expected to find the most stable structure, we found for each  $n$  that the three distinct optimized structures with lowest energies had very similar  $\text{CH}_3\text{NH}_2/\text{CO}_2$  structural features with the neighboring water molecules. Secondly, to simulate methylamine–carbon dioxide interactions in the presence of crystalline water ice, we performed geometry optimizations where the water initial geometry was taken as a fragment of the low temperature (less than 72 K) water ice XI phase which has an orthorhombic crystal structure. The ice XI unit cell contains 8 water molecules and has dimensions  $a = 4.5019$ ,  $b = 7.7978$ ,  $c = 7.3280$  Å.<sup>47</sup> We created a three layer ice slab containing 52 waters using the Avogadro advanced molecular editor<sup>48</sup> and the ice XI unit cell parameters. We then optimized several initial geometries generated with  $\text{CH}_3\text{NH}_2/\text{CO}_2$  absorbed at different positions above the slab. From the optimized  $\text{CH}_3\text{NH}_2/\text{CO}_2/(\text{H}_2\text{O})_{52}$  structure

with lowest energy we generated several more initial geometries with 14 and 30 additional waters randomly arranged above the  $\text{CH}_3\text{NH}_2/\text{CO}_2/(\text{H}_2\text{O})_{52}$  surface and then optimized these structures.

All of the geometry optimization and vibrational frequency calculations were performed using the GAMESS program suite.<sup>49</sup> Since performing these calculations using highly correlated methods and/or large basis sets is not practical for our large structures, we used B3LYP density functional theory calculations (DFT)<sup>50–52</sup> with the 6-31G(d) basis set.<sup>53</sup> To assess the reliability of 6-31G(d) basis for our system, we additionally performed calculations on related structures using the 6-311++G(d,p) basis set<sup>54,55</sup> on the  $\text{CH}_3\text{NH}_2/\text{CO}_2/(\text{H}_2\text{O})_n$  clusters containing up to 8 water molecules. Generally we found the 6-31G(d) and 6-311++G(d,p) basis sets to produce qualitatively similar geometries. Since the main goal of the present study is investigate  $\text{CH}_3\text{NH}_2/\text{CO}_2$  structural and vibrational frequency changes with an increasing number of water in the clusters, we considered the 6-31G(d) basis set as a good compromise for providing computational speed with chemical accuracy. Consequently, all of the electronic structure calculations on the larger  $\text{CH}_3\text{NH}_2/\text{CO}_2/(\text{H}_2\text{O})_n$  cluster with  $n > 8$  were performed at the B3LYP/6-31G(d) level. The large  $\text{CH}_3\text{NH}_2/\text{CO}_2/(\text{H}_2\text{O})_n$  clusters, which simulate the water structure in a crystalline phase with  $n \geq 52$ , contained too many atoms to facilitate a large number of different structures to be fully explored with calculations at the B3LYP/6-31G(d) level. To reduce the computational effort we replaced some of the water molecules at the cluster edges, and which were not expected to be directly interacting with or hydrogen bonding to the  $\text{CH}_3\text{NH}_2/\text{CO}_2$  complex, with effective fragment potentials (EFP).<sup>56–59</sup> In the EFP method the chemically inert part (there is no covalent bond breaking process) of the system is replaced by EFP while a regular DFT calculation with contributions from the EFP is performed for the chemically active part such as  $\text{CH}_3\text{NH}_2/\text{CO}_2$  with at least the neighboring water molecules. In our calculations we included the surface (upper) layer of the 3-layer ice slab, the  $\text{CH}_3\text{NH}_2/\text{CO}_2$  and any other surface water molecules with DFT, and replaced the lower two water layers with the water EFP. Thus in this EFP approach we take the lower two water layers to be inert where the water molecules only interact with each other and the active part through non-bonded interactions. These non-bonding interactions in van der Waals or hydrogen bonded complexes are implemented in the EFP method as: (a) coulombic interactions between fragments, and fragments with quantum mechanical molecules, (b) polarization or induction interaction between fragments, and fragments with quantum mechanical molecules, (c) exchange repulsion and charge transfer terms.<sup>56,60–62</sup> The electrostatic potential of the fragment is included as an additional one-electron term in the quantum mechanical Hamiltonian used in the active part of the system.<sup>57</sup> Effective fragments have frozen internal geometries. Therefore, they only rotate and translate as they interact with the part of the system treated by the DFT calculation and with each other, but their internal structures do not change during the optimizations. In the  $\text{CH}_3\text{NH}_2/\text{CO}_2$  structure determination calculations the lower two layers with the water EFP were constrained and the positions of

fragments were kept fixed while the upper layer was fully optimized. In our ice calculations, we again performed geometry optimizations and vibrational frequency calculations at the B3LYP/6-31G(d) level. For the EFP part of ice, we chose original EFP1/DFT (specifically, B3LYP) potential<sup>59</sup> which is a fitted repulsive potential for water fragments available in GAMESS.<sup>49</sup> After the geometry optimizations were completed, we performed vibrational frequency calculations on the optimized geometries to verify they were proper local minimum and to obtain estimates for the  $\text{CH}_3\text{NH}_2/\text{CO}_2$  complex IR vibrational spectra.

### 3. Results and discussion

#### 3.1 Structural analysis

**3.1.1 Methylamine and carbon dioxide complex in amorphous water clusters.** In this first subsection we describe the optimized geometries we obtained for the clusters where methylamine interacts with carbon dioxide in the presence of water molecules with an amorphous structure. In principle, the methylamine and carbon dioxide interactions might be expected to be the source for producing the neutral or zwitterionic forms of either the simple amino acid glycine or its isomer methylcarbamic acid in extraterrestrial ices. We performed geometry optimization calculations at the B3LYP/6-31G(d) level using different starting geometries on  $\text{CH}_3\text{NH}_2/\text{CO}_2/(\text{H}_2\text{O})_n$  clusters with  $n = 0, 1-4, 6, 8, 10, 12, 14, 16, 18$  and 20. Fig. 1 shows a schematic representation of the atom numbering used throughout the paper for the  $\text{CH}_3\text{NH}_2/\text{CO}_2$  complex and the neighboring water molecules which hydrogen bond with the complex. The lowest energy fully optimized  $\text{CH}_3\text{NH}_2/\text{CO}_2/(\text{H}_2\text{O})_n$  structures obtained for each  $n$  are presented in Fig. 2.

We found that in all of the optimized  $\text{CH}_3\text{NH}_2/\text{CO}_2/(\text{H}_2\text{O})_n$  structures the carbon dioxide favored being closest to the amino end of the methylamine. During the geometry optimizations, we found two different stable arrangements where the carbon

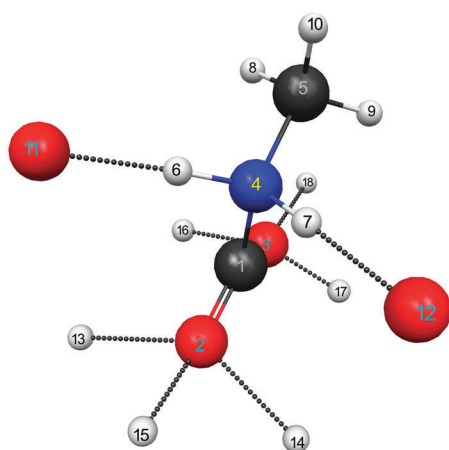


**Fig. 1** Atom labeling scheme used for the methylamine–carbon dioxide complex and neighboring atoms from the water environment. The numbering scheme is: O(2)–C(1)–O(3) for carbon dioxide, H(6)–N(4)–H(7) for the amine and C(5) with H(8), H(9) and H(10) for the methyl groups in methylamine; and O(11), O(12) and H(13) to H(18) are atoms on the surrounding water molecules which hydrogen bond to the complex.

dioxide was either *parallel* or *perpendicular* to the C(5)–N(4) bond direction of methylamine. The  $\text{CH}_3\text{NH}_2/\text{CO}_2/(\text{H}_2\text{O})_n$  structures with  $n = 2, 3$  with carbon dioxide perpendicular to the C(5)–N(4) bond were found to be slightly more stable [1.3 (Fig. 2c') and 4.6 (Fig. 2d')  $\text{kJ mol}^{-1}$ , respectively] than the parallel carbon dioxide conformers. In all of the other structures, the parallel carbon dioxide conformers were always found to be lower in energy. When we compared the average of C(1)–O(2) and C(1)–O(3) bond lengths for the different perpendicular and parallel type of conformers in  $\text{CH}_3\text{NH}_2/\text{CO}_2/(\text{H}_2\text{O})_n$  clusters, we obtained similar average C–O distances for the two conformers with the same  $n$ . It should be noted that with our geometry optimization strategy we did not expect to find the global minimum for these clusters, but we felt the structural features of these local minima should provide useful insights into how the geometry of the  $\text{CH}_3\text{NH}_2/\text{CO}_2$  complex evolves as the number of surrounding water molecules increases. In some of our calculations, we also found some even lower energy  $\text{CH}_3\text{NH}_2/\text{CO}_2/(\text{H}_2\text{O})_n$  structures, but these structures did not have direct interactions between methylamine and carbon dioxide molecules. Consequently, we do not discuss these structures further here as they do not provide any useful insights into the  $\text{CH}_3\text{NH}_2/\text{CO}_2$  interaction.

Without any water molecules present (Fig. 2a), we calculated the N(4)–C(1) distance between the methylamine N(4) atom and the carbon dioxide C(1) atom to be 2.808 Å and this value is consistent with a van der Waals complex being formed. Tabulated C and N van der Waals radii are 1.55 Å and 1.70 Å, respectively,<sup>63</sup> and the C(1) atom of carbon dioxide presumably favors interacting with the electron lone pair on the N(4) atom in methylamine. Our geometry is consistent with the previous N–C literature values which were calculated to range from 2.634 and 2.941 Å at different levels of theory for the methylamine–carbon dioxide interaction.<sup>27,29,42</sup> In addition, we found the carbon dioxide to be slightly bent with an angle of 175° also in agreement with the previously reported values between 175.8° and 176.7°.<sup>27,42</sup>

Fig. 2 shows that appreciable changes in the  $\text{CH}_3\text{NH}_2/\text{CO}_2$  geometry take place as the water molecules are added to the cluster and Table 1 summarizes the numerical geometrical parameters obtained for  $\text{CH}_3\text{NH}_2/\text{CO}_2$  in each water cluster. For comparison we also included the B3LYP/6-31G(d) optimized methylcarbamic acid geometrical parameters. Not too surprisingly, we obtained the lowest energy optimized structure with the water molecules preferring to be around the polar end of the complex. It was only after optimizing the  $\text{CH}_3\text{NH}_2/\text{CO}_2/(\text{H}_2\text{O})_{14}$  cluster that any water molecules were located in vicinity of the methyl group. Table 1 shows that the N(4)–C(1) distance between the amino group and carbon dioxide is a primary measure, and the carbon dioxide bond angle, O(2)–C(1)–O(3), a secondary measure, for how the interactions between methylamine and carbon dioxide change with an increasing number of surrounding water molecules.

*CH<sub>3</sub>NH<sub>2</sub>/CO<sub>2</sub>/H<sub>2</sub>O.* When one water molecule was added to the  $\text{CH}_3\text{NH}_2/\text{CO}_2$  complex and optimized, the N(4)–C(1) distance was shortened to 2.691 Å and the carbon dioxide bond angle became slightly more bent by 8°. Fig. 2b shows that the water acts as a hydrogen bond bridge between carbon

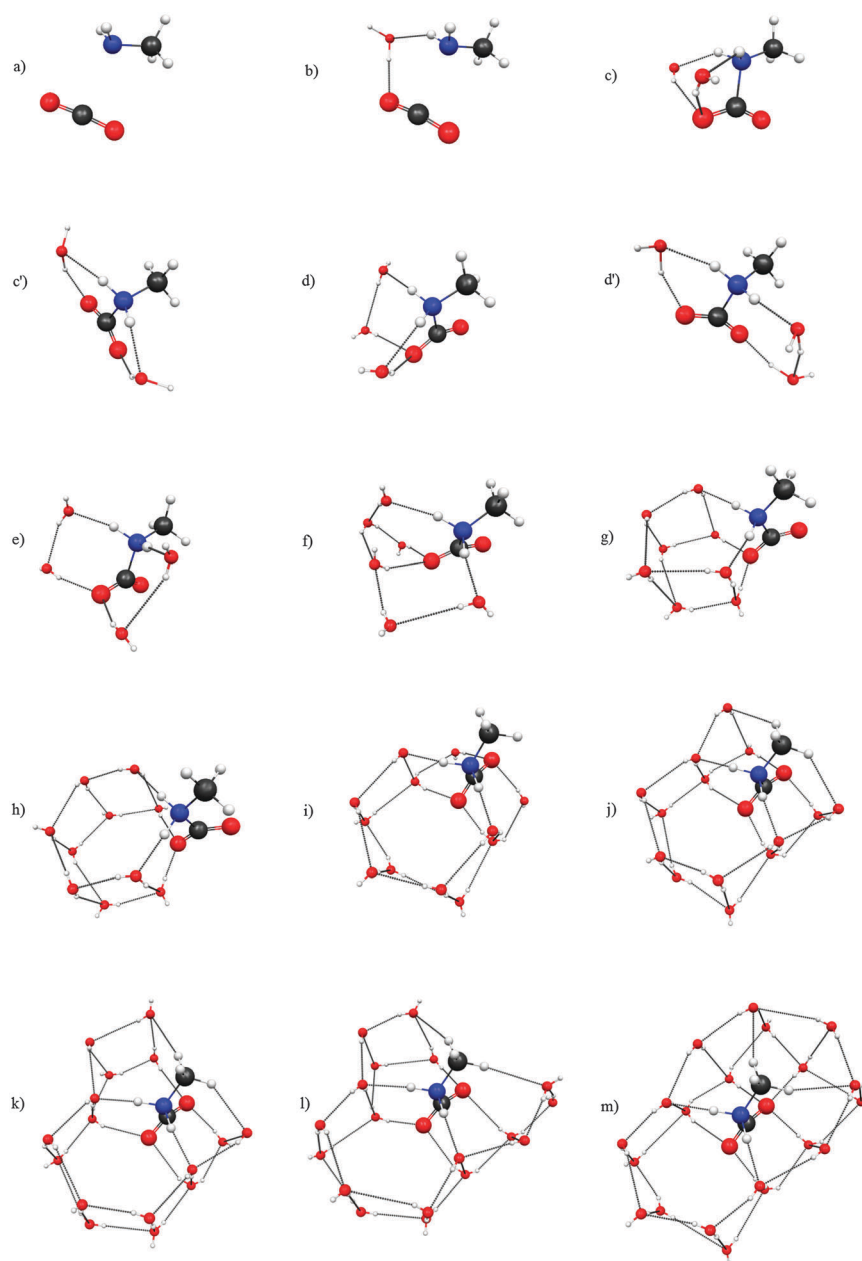


**Fig. 2** Optimized  $\text{CH}_3\text{NH}_2/\text{CO}_2/(\text{H}_2\text{O})_n$  cluster geometries obtained with amorphous water. The number of water molecules  $n$  in the clusters are zero (a), one (b), two (c and c'), three (d and d'), four (e), six (f), eight (g), ten (h), twelve (i), fourteen (j), sixteen (k), eighteen (l) and twenty (m). For clarity, the atoms in the water molecules are represented by using smaller spheres.

dioxide and methylamine and formed two hydrogen bonds with the complex: the water O(11) atom with the H(6) atom on the methylamine (2.124 Å) and the water H(1) atom with the O(2) atom on carbon dioxide (2.091 Å). The water serves as a proton acceptor from the amine group on methylamine and a proton donor to an oxygen atom on carbon dioxide.

$\text{CH}_3\text{NH}_2/\text{CO}_2/(\text{H}_2\text{O})_2$ . Fig. 2c and c' show dramatic changes took place in the  $\text{CH}_3\text{NH}_2/\text{CO}_2$  optimized structure when two water molecules were added to the complex. The conformer shown in Fig. 2c' is more stable than the conformer in Fig. 2c, but they only differ in energy by 1.3 kJ mol<sup>-1</sup>. In both structures the N(4)–C(1) distance was reduced by one

angstrom to 1.700 Å and the carbon dioxide became significantly bent with a bond angle of 140°. Both  $\text{CH}_3\text{NH}_2/\text{CO}_2/(\text{H}_2\text{O})_2$  conformers formed ring-type structures where again each water acted as a hydrogen bond bridge between the methylamine and carbon dioxide. In the structure shown in Fig. 2c both waters hydrogen bond to just the O(2) oxygen atom in carbon dioxide [H(14)–O(2) = 1.935 Å and H(13)–O(2) = 1.980 Å], whereas in Fig. 2c' the two water molecules separately form a hydrogen bond with the different oxygen atoms in carbon dioxide [H(13)–O(2) = H(17)–O(3) = 1.882 Å]. All of these hydrogen bond distances are shorter than those in the  $\text{CH}_3\text{NH}_2/\text{CO}_2/\text{H}_2\text{O}$  optimized structure suggesting that the hydrogen bonds in  $\text{CH}_3\text{NH}_2/\text{CO}_2/(\text{H}_2\text{O})_2$  are stronger.

**Table 1** Geometrical parameters (bond lengths in Å and bond angles in °) for the methylamine–carbon dioxide complex in the amorphous water clusters, the crystalline water clusters CWI, CWII and CWIII, and for reference the gas phase methylcarbamic acid (MCA, CH<sub>3</sub>NHCOOH), the ions CH<sub>3</sub>NH<sub>2</sub><sup>+</sup>COOH, CH<sub>3</sub>NHCOO<sup>-</sup> along with CO<sub>2</sub> and CO<sub>2</sub><sup>-a</sup>

Number of water	Carbon dioxide (CO <sub>2</sub> )			NH <sub>2</sub> –CO <sub>2</sub> N(4)–C(1)	CO <sub>2</sub> –CH <sub>3</sub> C(1)–C(5)	NH <sub>2</sub> –CH <sub>3</sub> N(4)–C(5)
	O(2)–C(1)–O(3)	C(1)–O(2)	C(1)–O(3)			
0	175.1	1.170	1.171	2.808	3.606	1.467
1	172.1	1.176	1.168	2.691	3.544	1.466
2	140.1	1.238	1.206	1.700	2.686	1.473
3	137.8	1.248	1.208	1.646	2.633	1.477
4	135.8	1.255	1.211	1.602	2.597	1.480
6	135.8	1.252	1.211	1.604	2.593	1.480
8	133.0	1.271	1.211	1.555	2.560	1.481
10	132.7	1.273	1.212	1.548	2.553	1.481
12	130.6	1.252	1.241	1.513	2.545	1.482
14	130.6	1.253	1.241	1.515	2.555	1.492
16	131.4	1.250	1.238	1.528	2.564	1.492
18	132.2	1.250	1.233	1.539	2.571	1.490
20	130.0	1.246	1.245	1.512	2.550	1.490
CWI	141.0	1.220	1.216	1.707	2.677	1.478
CWII	133.1	1.250	1.225	1.554	2.534	1.489
CWIII	131.1	1.260	1.228	1.523	2.516	1.500
MCA	123.1	1.368	1.219	1.358	2.462	1.450
CH <sub>3</sub> NH <sub>2</sub> <sup>+</sup> COOH	133.4	1.317	1.185	1.540	2.554	1.511
CH <sub>3</sub> NHCOO <sup>-</sup>	131.0	1.255	1.255	1.477	2.500	1.445
CO <sub>2</sub>	180	1.169	1.169			
CO <sub>2</sub> <sup>-</sup>	133.7	1.253	1.253			

<sup>a</sup> The atom labeling scheme is shown in Fig. 1.

Clearly the short 1.700 Å N(4)–C(1) distance indicates that the CH<sub>3</sub>NH<sub>2</sub>/CO<sub>2</sub>/(H<sub>2</sub>O)<sub>2</sub> cluster no longer forms just a van der Waals complex with a 2.808 Å N(4)–C(1) distance. This short N(4)–C(1) distance must arise from the greater amount of hydrogen bonding from the two water molecules, which in turn produces a stronger direct methylamine to carbon dioxide interaction. The optimized CH<sub>3</sub>NH<sub>2</sub>/CO<sub>2</sub>/(H<sub>2</sub>O)<sub>2</sub> geometry suggests an electron from the lone pair on the nitrogen atom is donated to the carbon dioxide, thereby enabling a N(4)–C(1) bond to be formed in a zwitterionic complex of the form CH<sub>3</sub>NH<sub>2</sub><sup>+</sup>–CO<sub>2</sub><sup>-</sup>. The 1.700 Å N(4)–C(1) distance appears to be relatively long to be as a covalent bond between the two atoms when compared against the 1.358 Å computed for the N–C distance in methylcarbamic acid. Nonetheless, the optimized geometries for the gas phase ions CH<sub>3</sub>NH<sub>2</sub><sup>+</sup>CO<sub>2</sub>H and CH<sub>3</sub>NHCO<sub>2</sub><sup>-</sup> show a lengthening of the N(4)–C(1) distance to 1.540 Å and 1.477 Å (Table 1), respectively, supporting the idea that a N(4)–C(1) bond is formed in the CH<sub>3</sub>NH<sub>2</sub>/CO<sub>2</sub>/(H<sub>2</sub>O)<sub>2</sub> cluster. Furthermore, when we performed a Mulliken (Lowdin) population analysis on the B3LYP Kohn–Sham orbitals for the CH<sub>3</sub>NH<sub>2</sub>/CO<sub>2</sub>/(H<sub>2</sub>O)<sub>2</sub> cluster, we found that there is an appreciable electron transfer from the methylamine to carbon dioxide [0.34 *e* (0.44 *e*) and 0.32 *e* (0.42 *e*) for the geometries given by Fig. 2c and c', respectively] versus the negligible partial charge on carbon dioxide [0.02 *e* (0.04 *e*)] computed for the CH<sub>3</sub>NH<sub>2</sub>/CO<sub>2</sub> complex shown in Fig. 2a. There is also a rapid rise in the dipole moment from 2.12 Debye for the CH<sub>3</sub>NH<sub>2</sub>/CO<sub>2</sub> complex with no water to 5.16 Debye for the CH<sub>3</sub>NH<sub>2</sub>/CO<sub>2</sub>/(H<sub>2</sub>O)<sub>2</sub> complex in Fig. 2c'. In addition, we performed Pipek–Mezey orbital localization analysis<sup>64</sup> on the CH<sub>3</sub>NH<sub>2</sub>/CO<sub>2</sub> complex in the gas phase and in the presence of two water molecules and investigated the change in the

localized orbitals during the interaction of CH<sub>3</sub>NH<sub>2</sub> and CO<sub>2</sub>. The lone pair orbital on nitrogen in the gas phase (Fig. 3a) becomes a C–N bonding orbital when two waters are added to the system (Fig. 3b). These results suggest that the two waters enable the CH<sub>3</sub>NH<sub>2</sub> and CO<sub>2</sub> to combine to produce the zwitterionic form of methylcarbamic acid, CH<sub>3</sub>NH<sub>2</sub><sup>+</sup>CO<sub>2</sub><sup>-</sup>. In addition, we find as expected that one role of the water is to reduce the energy needed to remove an electron from CH<sub>3</sub>NH<sub>2</sub> and add an electron to CO<sub>2</sub>. For CH<sub>3</sub>NH<sub>2</sub>, we compute an ionization energy of 8.55 eV in the gas phase and 7.54 eV with two waters; whereas 1.35 eV is needed to add an electron to gas phase CO<sub>2</sub> which is reduced to 0.13 eV with two waters present. Thus we compute a 2.23 eV net energy reduction in favor of forming the ions in presence of two water molecules. However, these energy calculations need to be considered with caution because there are large error bars associated with the large conformational changes in the explicit water geometries as the neutral CH<sub>3</sub>NH<sub>2</sub> and CO<sub>2</sub> molecules become charged and because the resulting CO<sub>2</sub><sup>-</sup> geometry is bent with a 133.7° bond angle. The 0.05 Å increase in the average C–O bond length and 140.1° bond angle in carbon dioxide with two waters are also consistent with CO<sub>2</sub><sup>-</sup> starting to be formed.

To further evaluate whether the role of the bridging water molecules is just to pull the carbon dioxide and methylamine closer together, which then facilitates electron transfer from the methylamine to carbon dioxide, we performed an electronic structure calculation on the optimized CH<sub>3</sub>NH<sub>2</sub>/CO<sub>2</sub>/(H<sub>2</sub>O)<sub>2</sub> geometry but with the two waters removed. A possible alternative viewpoint is that the bridging water molecules cause a polarization of the CH<sub>3</sub>NH<sub>2</sub>/CO<sub>2</sub> complex necessary to facilitate the electron transfer. From our calculations we found that the energy of the CH<sub>3</sub>NH<sub>2</sub>/CO<sub>2</sub> structure from Fig. 2c' but without

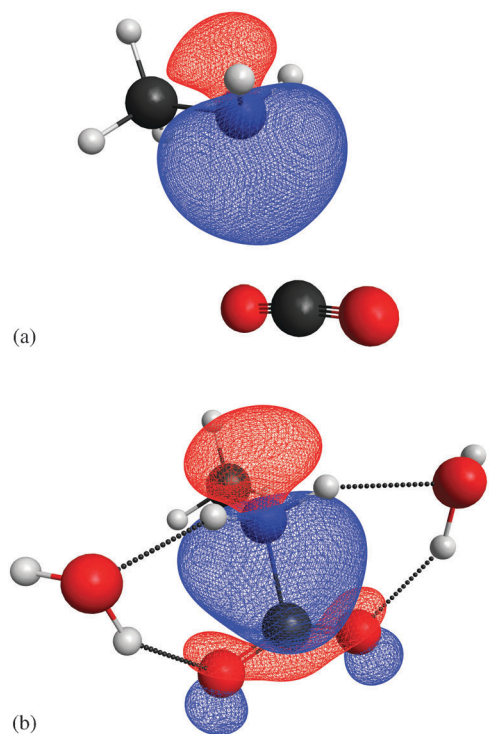


**Fig. 3** Localized orbitals showing the interaction between  $\text{CH}_3\text{NH}_2$  and  $\text{CO}_2$  (a) in the gas phase and (b) in the presence of two water molecules.

the 2 waters increased by  $62 \text{ kJ mol}^{-1}$  relative to the fully optimized  $\text{CH}_3\text{NH}_2/\text{CO}_2$  structure given in Fig. 2a. But we also found the unoptimized structure (Fig. 2c' without waters) to have a 6.72 D dipole moment and the Mulliken (Lowdin) population analysis net carbon dioxide charges [ $0.34 e$  ( $0.45 e$ )] much greater than the 2.13 D dipole and carbon dioxide charge [ $0.02 e$  ( $0.04 e$ )] for the optimized  $\text{CH}_3\text{NH}_2/\text{CO}_2$  van der Waals complex. These calculations support the idea that the bridging water molecules are responsible for bringing the carbon dioxide and methylamine closer together, and this then enables a substantial electron transfer from methylamine to carbon dioxide. A plot of the extent of electron transfer from methylamine to carbon dioxide as suggested by a population analysis against the number of water molecules is shown in Fig. 4a. Likewise the dipole moment variation computed for the  $\text{CH}_3\text{NH}_2/\text{CO}_2$  structure taken from the optimized  $\text{CH}_3\text{NH}_2/\text{CO}_2/(\text{H}_2\text{O})_n$  cluster shown in Fig. 4b is also consistent with electron transfer from methylamine to carbon dioxide when  $n = 2$ . We conclude that the two bridging water molecules are able to promote electron transfer thermally without requiring some electronic excitation process to stimulate the electron transfer.

$\text{CH}_3\text{NH}_2/\text{CO}_2/(\text{H}_2\text{O})_{3-12}$ . Including more waters, from 3 (Fig. 2d) to 12 (Fig. 2i), continues to more gently modify the  $\text{CH}_3\text{NH}_2/\text{CO}_2$  complex structure. In Fig. 5, we graphed the variation in the N(4)–C(1) distance between methylamine and carbon dioxide, the  $\text{CO}_2$  bond angle and the two C–O bond lengths as a function of the number of waters in the  $\text{CH}_3\text{NH}_2/\text{CO}_2/(\text{H}_2\text{O})_n$  complex. Fig. 5 shows the N(4)–C(1) distance decreases gradually from  $1.646 \text{ \AA}$  to  $1.515 \text{ \AA}$ , the

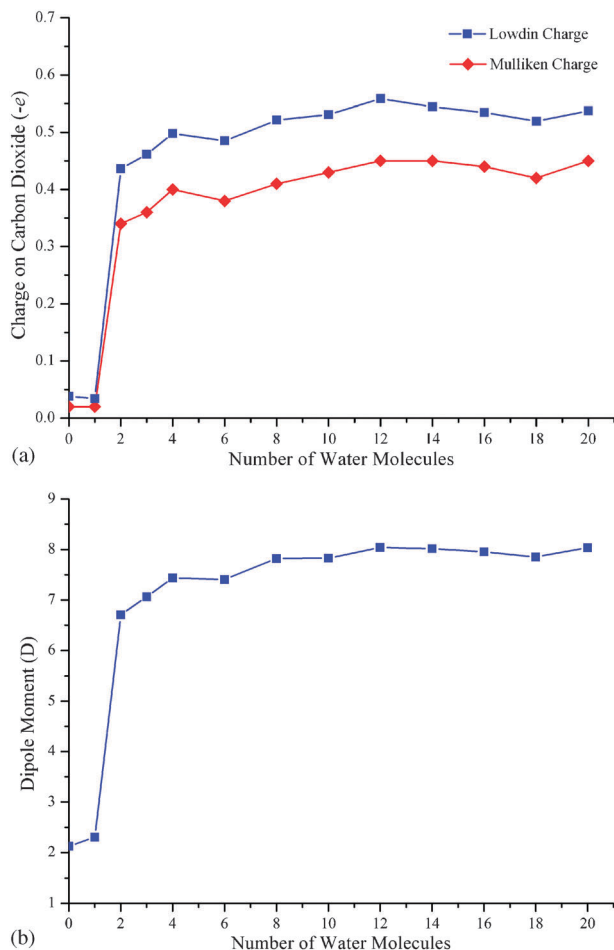


**Fig. 4** Variation of (a) the carbon dioxide net charges (in  $-e$ ) obtained by the Mulliken and Lowdin populations analyses, and (b)  $\text{CH}_3\text{NH}_2/\text{CO}_2$  dipole moment (in D) computed without the water present plotted against the number of water molecules in the  $\text{CH}_3\text{NH}_2/\text{CO}_2/(\text{H}_2\text{O})_n$  clusters.

carbon dioxide angle changes from  $138^\circ$  to  $131^\circ$ , and the C–O bond lengths are slightly lengthened on going from 3 to 12 waters. At the same time, both increases in the dipole moment (7.06 to 8.04 D) and the Mulliken (Lowdin) population analysis of carbon dioxide charge [ $0.36 e$  ( $0.46 e$ ) to  $0.45 e$  ( $0.56 e$ )] indicates the amount of electron transfer from the methylamine to carbon dioxide increases slightly after more than two waters are added to the cluster (Fig. 4). The carbon dioxide bond lengths and bond angles for  $n = 3$  to 20 are very similar to the  $1.253 \text{ \AA}$  C–O bond length and  $133.7^\circ$  O–C–O bond angle obtained by separately optimizing the  $\text{CO}_2^-$  anion at the B3LYP/6-31G(d) level. It is interesting to note the hydrogen bonding water bridges pulling carbon dioxide closer to methylamine in the  $\text{CH}_3\text{NH}_2/\text{CO}_2/(\text{H}_2\text{O})_n$  complexes with  $n > 2$  in some cases contain more than a single water molecule. For example, for three waters in Fig. 2d and d', one of the hydrogen bond bridges is made up from two water molecules, and the two hydrogen bond bridges between carbon dioxide and methylamine for the four water structure in Fig. 2e both consist of two water molecules. The presence of two waters in the hydrogen bonding bridge enables the N(4)–C(1) distance

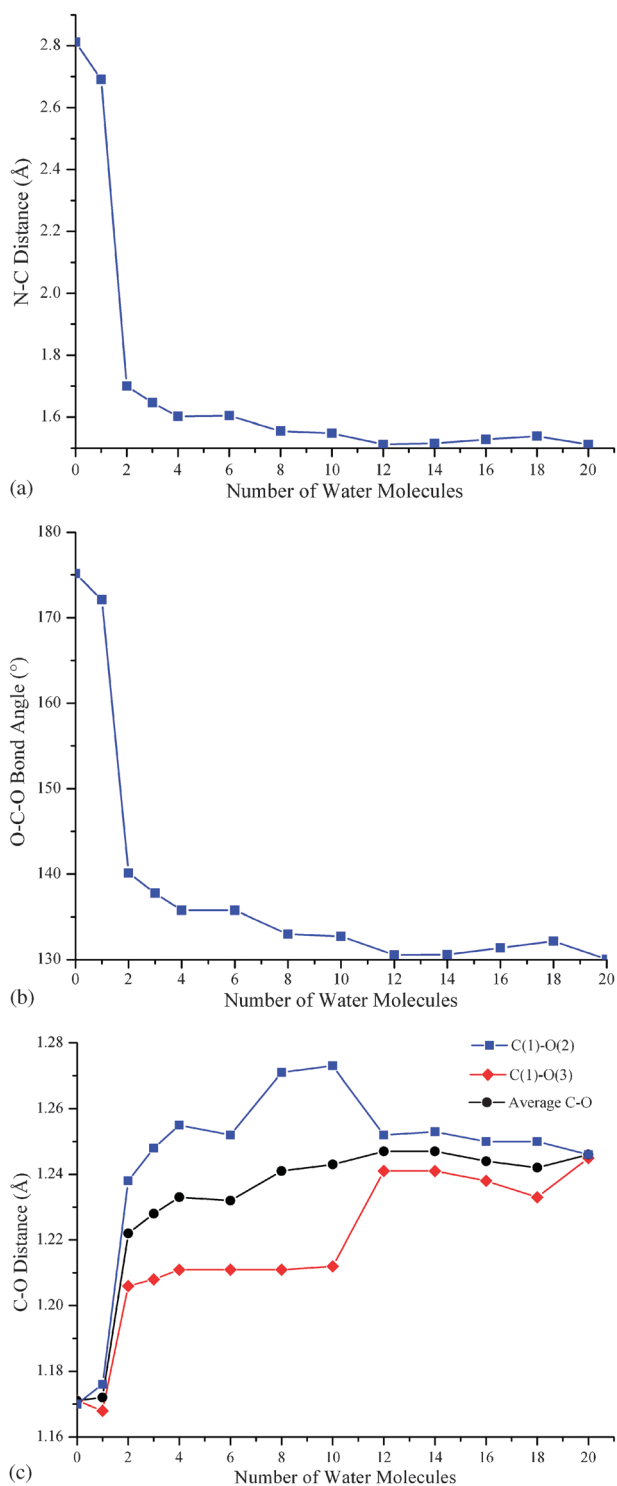


**Fig. 5** Graphs of (a) the methylamine–carbon distance given as the N(4)–C(1) distance (in Å), (b) the carbon dioxide bond angle (in °), and (c) the two C–O bond lengths and the average C–O distance in carbon dioxide (in Å) plotted against the number of water molecules in the  $\text{CH}_3\text{NH}_2/\text{CO}_2/(\text{H}_2\text{O})_n$  cluster.

to be shortened further from 1.700 Å ( $n = 2$ ) to 1.646 Å ( $n = 3$ ) and 1.602 Å ( $n = 4$ ).

$\text{CH}_3\text{NH}_2/\text{CO}_2/(\text{H}_2\text{O})_{14-20}$ . Table 1 and Fig. 5 show the  $\text{CH}_3\text{NH}_2/\text{CO}_2$  structure to remain essentially constant in the

clusters containing 14 (Fig. 2j) to 20 (Fig. 2m) water molecules. This is partly because the extra water molecules in the 14 to 20 structures are being added around the methyl end of methylamine and away from the region where the carbon dioxide interacts with methylamine. Nevertheless, we obtained the shortest N(4)–C(1) distance (1.512 Å) and the smallest carbon dioxide angle (130°) with the cluster containing 20 water molecules. Fig. 5c shows that there can be a fairly wide difference between the two C(1)–O(2) and C(1)–O(3) distances in carbon dioxide especially in the  $n = 2$  to 10 clusters. We attribute these differences to O(2) and O(3) atoms interacting with different numbers of surrounding water molecules and found the average C–O distance to increase smoothly to 1.25 Å when there are twenty water molecules in the cluster. In the  $n = 20$  case, the water molecule arrangement around each of the oxygen atoms on the bent  $\text{CO}_2$  causes the two C–O distances to be essentially the same. Fig. 6 summarizes the hydrogen bond distance variation with number of water molecules in the cluster. From Fig. 6 we again found initially large distance changes as the first 2 to 4 waters are added to the  $\text{CH}_3\text{NH}_2/\text{CO}_2$  complex, and then a more gentle variation in the hydrogen-bond lengths for the larger clusters.

Our calculations suggest that the bridging water molecules which form hydrogen bond bridges between methylamine and carbon dioxide appear to be facilitating a thermal electron transfer from methylamine to carbon dioxide to presumably end up with a methylcarbamic acid zwitterion of the form  $\text{CH}_3\text{NH}_2^+\text{CO}_2^-$ . There were a few examples of related systems reported previously: cyanamide–water  $[\text{NH}_2\text{CN}/(\text{H}_2\text{O})_n; n = 1-6]$ ,<sup>65</sup> dimethylamine–carbon dioxide  $[\text{((CH}_3)_2\text{NH)}_n/\text{CO}_2; n = 1, 2]$ ,<sup>43</sup> ammonia–carbon dioxide  $[(\text{NH}_3)_n/\text{CO}_2; n = 1, 2]$ ,<sup>66</sup> and methylamine–carbon dioxide  $[(\text{CH}_3\text{NH}_2)_n/\text{CO}_2; n = 1-3]$  systems<sup>29</sup> where one of the molecules acts as a hydrogen bond bridge molecule. One interesting aspect of the  $\text{CH}_3\text{NH}_2/\text{CO}_2/(\text{H}_2\text{O})_n$  cluster geometries is that the carbon dioxide becomes more bent as more waters are added to the clusters. This contrasts with carbon dioxide on its own in water clusters where the carbon dioxide essentially remains linear.<sup>44,45</sup> We discuss the consequences of the carbon dioxide bending on the vibrational frequencies for  $\text{CH}_3\text{NH}_2/\text{CO}_2/(\text{H}_2\text{O})_n$  in more detail below. We found the  $\text{CH}_3\text{NH}_2^+\text{CO}_2^-$  zwitterion is only stable in the presence of the surrounding water molecules. When we start a geometry optimization using an initial  $\text{CH}_3\text{NH}_2^+\text{CO}_2^-$  structure taken from one of the optimized  $\text{CH}_3\text{NH}_2/\text{CO}_2/(\text{H}_2\text{O})_n$  clusters but with the  $n$  water molecules removed we always obtain the van der Waals complex structure shown in Fig. 2a. A similar geometry optimization result was found for glycine, where the optimized glycine zwitterion is only computed when water molecules are hydrogen bonded to the glycine.<sup>37,40,67</sup> Finally, we note that in all of these calculations we never found a structure where a hydrogen atom spontaneously transferred from methylamine to carbon dioxide. Presumably this proton transfer will require, as proposed by others,<sup>40,41</sup> some excitation process, such as by UV or electron irradiation, before this can occur. However, the optimized structures we found from our calculations do suggest that the hydrogen bonded bridging waters could perhaps act as a shuttle for the proton transfer from methylamine to carbon dioxide.

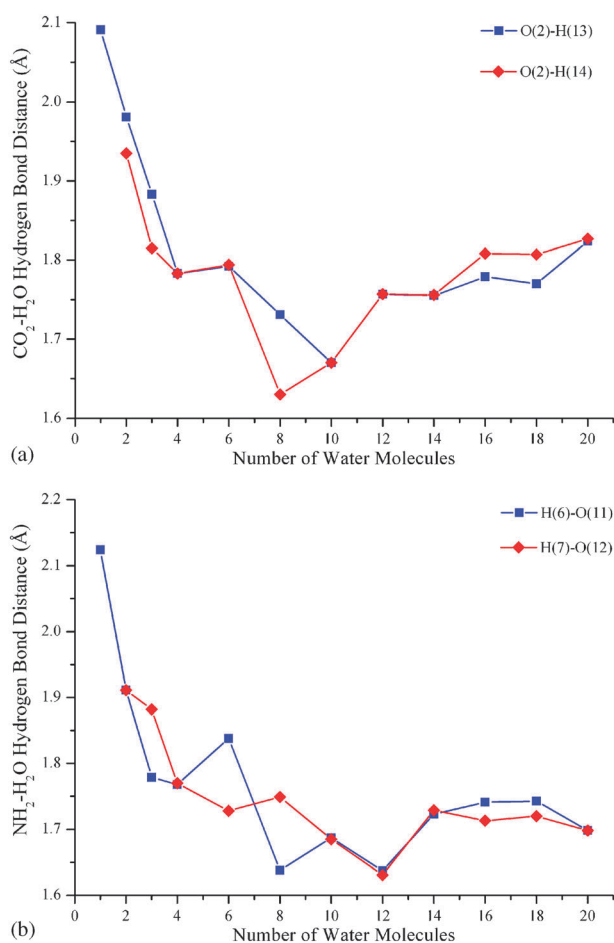


**Fig. 6** Variation of the hydrogen bond distance (in Å) between neighboring water molecules and (a) the oxygen atom on carbon dioxide and (b) the hydrogen atoms on the methylamine amine group.

### 3.1.2 Methylamine and carbon dioxide complex on a crystalline water–ice surface.

In this part, we report the results from the investigation of the CH<sub>3</sub>NH<sub>2</sub>/CO<sub>2</sub> complex adsorbed on a crystalline water–ice surface. We also considered the situation where there were enough additional water molecules to completely surround the CH<sub>3</sub>NH<sub>2</sub>/CO<sub>2</sub> complex on the ice surface. Although mostly the amorphous phase of water ice was previously considered in experimental studies and theoretical models of icy grain mantles,<sup>68–72</sup> Rimola *et al.*<sup>73</sup> and Allouche *et al.*<sup>74</sup> have used crystalline ice structures in their cluster calculations after making the assumption that amorphous ice can be regarded as being partially ordered on the molecular scale. As described in the Computational method section, we prepared a small fragment of the ice XI crystal structure composed of 52 water molecules arranged as a slab simulating the top 3-layers of the (100) ice XI surface built using geometry information based on the ice XI crystallographic data.<sup>47</sup> Initial guesses at the preferred CH<sub>3</sub>NH<sub>2</sub>/CO<sub>2</sub> complex adsorption geometry were made by placing the complex with a 3 Å N(4)–C(1) distance at different sites at approximately 5 Å above the surface. A partial geometry optimization calculation was performed on each CH<sub>3</sub>NH<sub>2</sub>/CO<sub>2</sub>/(H<sub>2</sub>O)<sub>n</sub> structure with  $n = 52$  (CWI), 66 (CWII), and 82 (CWIII) at the B3LYP/6-31G(d) level for methylamine, carbon dioxide and the water

surface layer of the ice slab, while 36 of the water molecules located in the lower two layers of the ice were treated using the EFP1/DFT potentials.<sup>59</sup> The geometries of the three structures were partially optimized by keeping the 36 EFP waters fixed at the experimental ice XI geometry and minimizing the clusters energy by relaxing the positions of all the other atoms which are included in the DFT calculation. We found the resulting optimized structures interesting in that, although the top surface layer of the ice can fully relax, the cluster retains most of its crystalline structure. Our approach is consistent with a previous study which found that when a full geometry optimization of a cluster simulating crystalline water is performed, the resulting geometry is dramatically deformed at the cluster edges due to the formation of extra hydrogen bonds not present in the bulk structure.<sup>73</sup>

*CWI.* Fig. 7 shows the resulting lowest energy optimized structure of CH<sub>3</sub>NH<sub>2</sub>/CO<sub>2</sub>/(H<sub>2</sub>O)<sub>52</sub> (CWI) containing the CH<sub>3</sub>NH<sub>2</sub>/CO<sub>2</sub> complex at its preferred adsorption site above the water–ice surface. We found that each of the oxygen atoms in carbon dioxide make a hydrogen bond with a water molecule in the ice surface and the amino group of methylamine also makes a hydrogen bond to an oxygen atom on a different water in the ice surface. We calculated the carbon dioxide O(2)–H(14), O(3)–H(16) and amino H(7)–O(12) hydrogen bonding distances to be 1.904 Å, 1.844 Å and 1.881 Å, respectively. A summary of the CH<sub>3</sub>NH<sub>2</sub>/CO<sub>2</sub> complex geometry contained in CWI is included in Table 1. The large 39° bending of the carbon dioxide bond angle and the average C–O distance of 1.218 Å along with the reduced carbon dioxide to methylamine separation to produce a N(4)–C(1) distance of 1.707 Å suggests that the geometry of CH<sub>3</sub>NH<sub>2</sub>/CO<sub>2</sub> complex within the CWI structure is very similar in nature to that occurring for the CH<sub>3</sub>NH<sub>2</sub>/CO<sub>2</sub>/(H<sub>2</sub>O)<sub>2</sub> amorphous cluster. An important difference in all the crystalline water clusters is that the carbon dioxide and methylamine can more readily form hydrogen bonds with several different water molecules. This contrasts with the hydrogen bonds in the amorphous clusters which have two or three water molecules which simultaneously hydrogen bond to both the carbon dioxide and methylamine molecules.

*CWII.* To investigate whether the interactions in the CH<sub>3</sub>NH<sub>2</sub>/CO<sub>2</sub> complex adsorbed on the ice surface become modified by the presence of extra surface waters we performed a geometry optimization on the CH<sub>3</sub>NH<sub>2</sub>/CO<sub>2</sub>/(H<sub>2</sub>O)<sub>66</sub> cluster (CWII) with 14 extra water molecules added to the CWI structure shown in Fig. 7. This number of extra waters in CWII was selected so as to enable the sides of the CH<sub>3</sub>NH<sub>2</sub>/CO<sub>2</sub> complex to be completely surrounded. Once again, we performed a geometry optimization using EFP1/DFT potentials for the fixed water molecules in the lower two layers of the ice and a B3LYP/6-31G(d) calculation for the rest of the system. The CWII optimized structure is shown in Fig. 8 with the CH<sub>3</sub>NH<sub>2</sub>/CO<sub>2</sub> complex geometry summarized in Table 1. The 14 additional waters formed a new ice layer with a hydrogen bonding network with the ice surface and also with the CH<sub>3</sub>NH<sub>2</sub>/CO<sub>2</sub>. Analogous to the CH<sub>3</sub>NH<sub>2</sub>/CO<sub>2</sub>/(H<sub>2</sub>O)<sub>n</sub> amorphous clusters, the additional water surrounding the

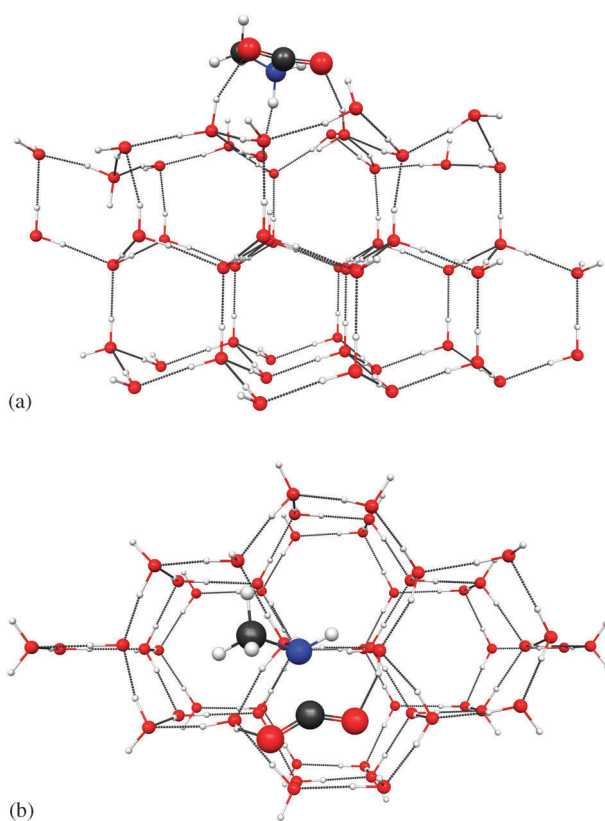


**Fig. 7** Adsorption of methylamine and carbon dioxide on top of the ice XI surface consisting of 16 waters and 36 EFP waters: (a) side-view, and (b) top-view. For clarity, the atoms in the water molecules are represented by using smaller spheres.

$\text{CH}_3\text{NH}_2/\text{CO}_2$  complex in CWII appears to make the interaction between the methylamine and carbon dioxide stronger. This is indicated by the much shorter N(4)–C(1) distance of 1.554 Å, a longer average 1.237 Å C–O distance and the smaller 133° bond angle relative to CWI. The N(4)–C(1) distance and the distorted carbon dioxide geometry in CWII suggest that the  $\text{CH}_3\text{NH}_2/\text{CO}_2$  complex resembles the amorphous cluster containing 8 waters given in Table 1.

*CWIII*. Finally, we formed the CWIII structure by adding 16 water molecules to the top layer of the CWII structure (or 30 to the CWI structure) and performed the same type of partial geometry optimization as before. The CWIII optimized geometry is shown in Fig. 9 and now has the  $\text{CH}_3\text{NH}_2/\text{CO}_2$  complex completely encapsulated in a hydrogen bonding network formed by the ice surface and the surrounding water molecules. Again, the fully trapped complex has a shorter N(4)–C(1) distance (1.523 Å), longer average C–O distance (1.248 Å) and smaller carbon dioxide angle (131°) than in the CWII structure suggesting that in CWIII the methylamine and carbon dioxide interact with each other more strongly than in CWII. The geometrical parameters of the CWIII structure given in Table 1, where the  $\text{CH}_3\text{NH}_2/\text{CO}_2$  complex is completely encapsulated by water molecules, resemble the complex in the amorphous cluster containing 16 water molecules.

Overall, we feel the trends in the  $\text{CH}_3\text{NH}_2/\text{CO}_2$  complex geometrical parameters summarized in Table 1 obtained from

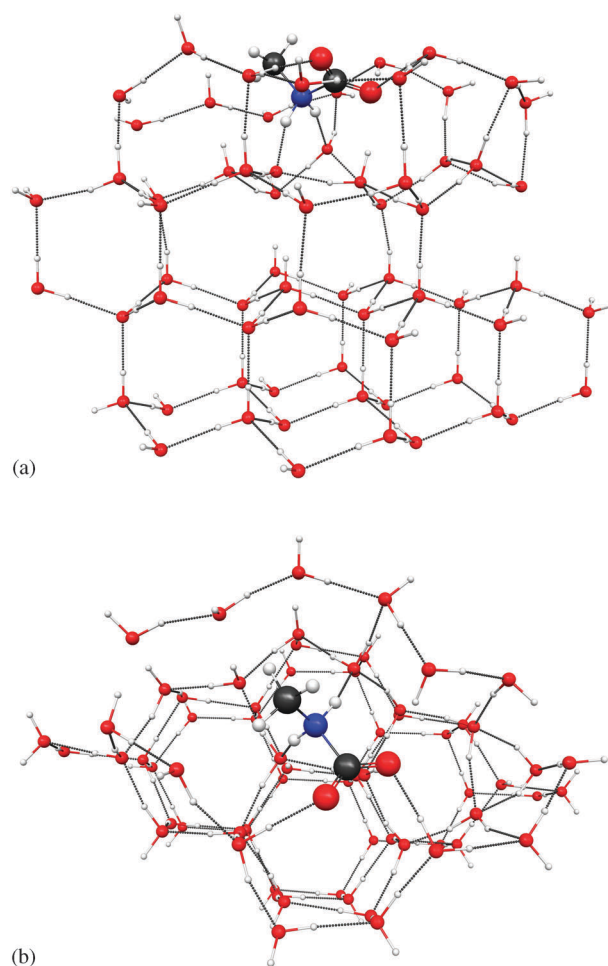


**Fig. 8** Methylamine–carbon dioxide in the top layer of the ice XI surface surrounded by 14 additional water molecules around the sides so that the cluster includes 30 waters and 36 EFP waters: (a) side-view, and (b) top-view. For clarity, the atoms in the water molecules are represented by using smaller spheres.

the calculations on the  $\text{CH}_3\text{NH}_2/\text{CO}_2/(\text{H}_2\text{O})_n$  clusters with amorphous water and the crystalline water demonstrate that the extent of the methylamine and carbon dioxide interaction mainly depends on the number of surrounding water neighbors. We found the  $\text{CH}_3\text{NH}_2/\text{CO}_2$  complex in the crystalline water clusters CWI, CWII and CWIII to resemble the amorphous clusters containing  $n = 2, 8$  and 16 waters, respectively, indicating that the N(4)–C(1) distance is not governed by a specific type of hydrogen bonding bridge formed by one or more water molecules. This also suggests that forming the  $\text{CH}_3\text{NH}_2/\text{CO}_2$  complex is not sensitive to being in an amorphous or crystalline water environment. Dipole moment calculations, where the surrounding water molecules are removed, gave 6.63, 7.80, 8.07 Debye, respectively, for the CWI, CWII and CWIII optimized  $\text{CH}_3\text{NH}_2/\text{CO}_2$  complexes. Both the dipole moment calculations and the Mulliken and Lowdin population analyses are consistent with a large electron transfer from the methylamine to carbon dioxide taking place to produce the methylcarbamic acid zwitterion  $\text{CH}_3\text{NH}_2^+\text{CO}_2^-$  in the crystalline water ice structures.

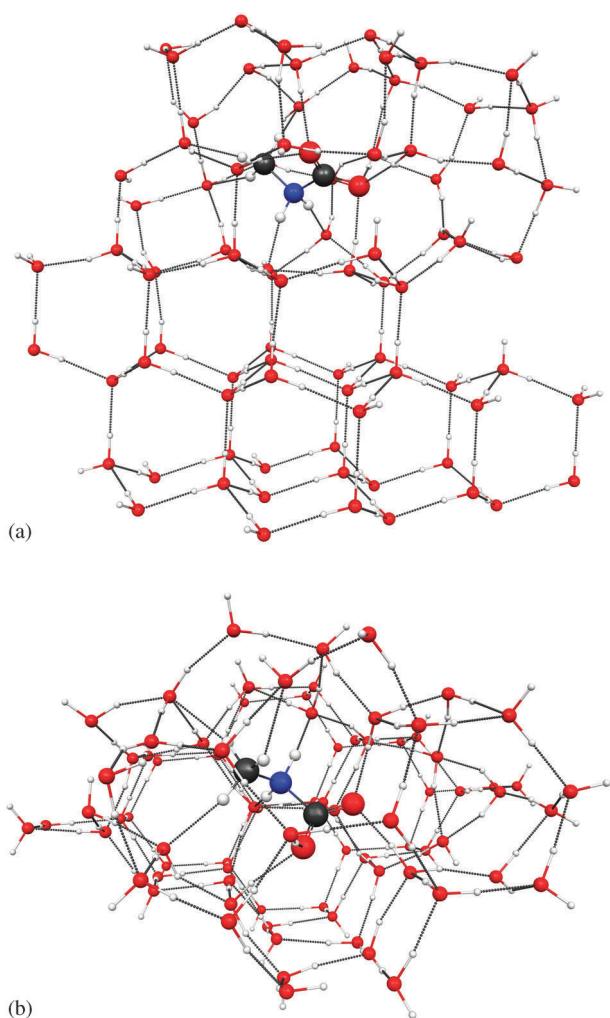


**Fig. 9** Methyamine-carbon dioxide trapped encapsulated in ice formed from 46 waters and 36 EFP waters: (a) side-view, and (b) top-view. For clarity, the atoms in the water molecules are represented by using smaller spheres.

### 3.2 Vibrational frequency analysis

In this section, we present the results from B3LYP/6-31G(d) vibrational frequency calculations on the geometry optimized amorphous and crystalline  $\text{CH}_3\text{NH}_2/\text{CO}_2(\text{H}_2\text{O})_n$  clusters described in the last two subsections. Table 2 summarizes the frequencies computed for isolated methylamine and carbon dioxide molecules (in column 3), the  $\text{CH}_3\text{NH}_2/\text{CO}_2$  van der Waals complex (column 4) and the two  $\text{CH}_3\text{NH}_2/\text{CO}_2/(\text{H}_2\text{O})_2$  (columns 5 and 6) conformers. Also included in Table 2 are the experimentally observed IR active vibrational frequencies of Holtom *et al.*<sup>27</sup> and Bossa *et al.*<sup>75</sup> for methylamine-carbon dioxide binary ice mixtures at 10 K. In the following discussion we used the computed vibrational frequencies as directly obtained from the B3LYP/6-31G(d) calculations rather than with a 0.96 scaling factor often used to compensate for the theoretical frequencies tending to be systematically higher than the experimental values.<sup>76</sup> The computed fundamental vibrations in Table 2 from the calculations on the individual methylamine and carbon dioxide molecules essentially simulate the frequencies observed for the isolated molecules in the gas phase. The computed

carbon dioxide fundamentals correlated well with the experimental gas phase vibrations (IR active intense asymmetric stretch  $2349\text{ cm}^{-1}$  and bending  $667\text{ cm}^{-1}$ , and the IR inactive symmetric stretch  $1333\text{ cm}^{-1}$ ).<sup>76</sup> Likewise, the computed fundamentals for the isolated methylamine generally agreed well with the previous experimental IR active frequency assignments listed in Table 2 obtained for solid methylamine.<sup>27,75</sup> Perhaps the major discrepancy in the computed frequencies for the isolated methylamine molecule occurred for the  $\text{NH}_2$   $\nu_1$  symmetric and  $\nu_{10}$  asymmetric stretches where they exceed the experimental frequency values by approximately  $200\text{ cm}^{-1}$ . But as we discuss below, these computed  $\text{NH}_2$  stretching frequencies become much closer in agreement with the experimental values in the  $\text{CH}_3\text{NH}_2/\text{CO}_2/(\text{H}_2\text{O})_n$  complexes when water molecules form hydrogen bonds with the  $\text{NH}_2$  groups.

**$\text{CH}_3\text{NH}_2/\text{CO}_2$ .** In the  $\text{CH}_3\text{NH}_2/\text{CO}_2$  van der Waals complex (Fig. 2a) there is still a relatively large separation between the carbon dioxide and methylamine, and consequently there are only small shifts ( $<20\text{ cm}^{-1}$ ) in the vibrational frequencies from those for the isolated carbon dioxide and methylamine molecules. The slight  $5^\circ$  distortion from linear carbon dioxide in the complex caused the doubly degenerate  $640\text{ cm}^{-1}$  bending mode to split into a bending mode ( $647\text{ cm}^{-1}$ ) in the carbon dioxide plane and an out-of-plane bending mode ( $595\text{ cm}^{-1}$ ) which are both IR active. Since the carbon dioxide is no longer linear, the out-of-plane bending mode more strictly corresponds to a frustrated carbon dioxide rotation which couples with vibrational modes involving the nitrogen atom of methylamine to produce an IR active band with a greater intensity ( $1.5 \times 10^{-17}\text{ cm molecule}^{-1}$ ) than the in-plane carbon dioxide bending vibration ( $0.5 \times 10^{-17}\text{ cm molecule}^{-1}$ ). Another important consequence of the carbon dioxide bending is that the originally IR inactive carbon dioxide symmetric stretch at  $1371\text{ cm}^{-1}$  starts to become weakly IR active ( $0.05 \times 10^{-17}\text{ cm molecule}^{-1}$ ) in the  $\text{CH}_3\text{NH}_2/\text{CO}_2$  complex.

**$\text{CH}_3\text{NH}_2/\text{CO}_2/(\text{H}_2\text{O})_2$ .** The fifth and sixth columns in Table 2 list the computed frequencies for the parallel and perpendicular conformers of the  $\text{CH}_3\text{NH}_2/\text{CO}_2/(\text{H}_2\text{O})_2$  complex. This complex can be regarded as a prototype for the larger interactions which take place between methylamine and carbon dioxide in the presence of several water molecules in a low temperature ice. As we have already noted, the two water molecules draw the carbon dioxide approximately an Å closer to the nitrogen atom in methylamine. The resulting larger methylamine and carbon dioxide interaction seems to mostly affect the carbon dioxide vibrational modes. The carbon dioxide asymmetric stretch remains strongly IR active but is *drastically red shifted* by  $435\text{ cm}^{-1}$  to  $1989\text{ cm}^{-1}$ . The carbon dioxide symmetric stretch is less strongly red shifted by  $75\text{ cm}^{-1}$  to  $1289\text{ cm}^{-1}$ , however, since the O-C-O angle is now bent to  $140^\circ$  there is a huge increase in the  $\nu_s$  IR band intensity. The carbon dioxide bending mode is blue shifted in the parallel (perpendicular) conformers by  $30\text{ cm}^{-1}$  ( $76\text{ cm}^{-1}$ ). The different symmetries of the two  $\text{CH}_3\text{NH}_2/\text{CO}_2/(\text{H}_2\text{O})_2$  structures result in a much larger bending vibration IR intensity in the perpendicular *versus* the parallel  $\text{CO}_2$  conformer.

**Table 2** Computed and experimental IR absorption frequencies ( $\text{cm}^{-1}$ ) of the isolated methylamine ( $\text{CH}_3\text{NH}_2$ ) and carbon dioxide ( $\text{CO}_2$ ), the methylamine–carbon dioxide complex ( $\text{CH}_3\text{NH}_2/\text{CO}_2$ ) and the methylamine–carbon dioxide complex with two waters [ $\text{CH}_3\text{NH}_2/\text{CO}_2/(\text{H}_2\text{O})_2$ ]. The IR intensities ( $\times 10^{-17}$   $\text{cm molecule}^{-1}$ ) are given in parentheses

Assignment/characterization	Molecule	Isolated $\text{CH}_3\text{NH}_2$ and $\text{CO}_2$	$\text{CH}_3\text{NH}_2/\text{CO}_2$ complex	$\text{CH}_3\text{NH}_2/\text{CO}_2/(\text{H}_2\text{O})_2$ complex <sup>a</sup>	$\text{CH}_3\text{NH}_2/\text{CO}_2$ complex, experimental <sup>b</sup>	$\text{CH}_3\text{NH}_2/\text{CO}_2$ complex, experimental <sup>c</sup>	
$\nu_{10}$ $\text{NH}_2$ asymmetric stretch	$\text{CH}_3\text{NH}_2$	3556 (0.01)	3552 (0.001)	3312 (5.3)	3299 (8.4)	—	3334
$\nu_1$ $\text{NH}_2$ symmetric stretch	$\text{CH}_3\text{NH}_2$	3463 (0.04)	3470 (0.01)	3237 (4.6)	3231 (2.1)	3296	3282
$\nu_{11}$ $\text{CH}_3$ asymmetric stretch	$\text{CH}_3\text{NH}_2$	3117 (0.6)	3129 (0.5)	3194 (0.4)	3171 (0.3)	3001, 2995	2967, 2942, 2929
$\nu_2$ $\text{CH}_3$ asymmetric stretch	$\text{CH}_3\text{NH}_2$	3077 (0.8)	3090 (0.6)	3158 (0.2)	3151 (0.3)	2950	2897, 2883, 2862
$\nu_3$ $\text{CH}_3$ symmetric stretch	$\text{CH}_3\text{NH}_2$	2969 (1.7)	2989 (1.6)	3083 (0.5)	3074 (0.4)	2798	2808, 2792
$\nu_3$ $\text{CO}_2$ asymmetric stretch	$\text{CO}_2$	2435 (9.1)	2424 (8.4)	1989 (9.1)	1988 (9.8)	2363	2327
$\nu_3$ $^{13}\text{CO}_2$ isotope peak	$^{13}\text{CO}_2$	2365 (8.4)	2355 (7.7)	1933 (8.4)	1933 (9.1)	2282	2281
$\nu_4$ $\text{NH}_2$ sciss	$\text{CH}_3\text{NH}_2$	1703 (0.4)	1701 (0.4)	1723 (0.4)	1689 (0.4)	1594	1615
$\nu_5$ $\text{CH}_3$ asymmetric deformation	$\text{CH}_3\text{NH}_2$	1548 (0.04)	1546 (0.07)	1525 (0.2)	1531 (0.3)	1504	—
$\nu_{12}$ $\text{CH}_3$ asymmetric deformation	$\text{CH}_3\text{NH}_2$	1528 (0.1)	1526 (0.07)	1520 (0.1)	1535 (0.3)	1475	1477, 1455
$\nu_6$ $\text{CH}_3$ symmetric deformation	$\text{CH}_3\text{NH}_2$	1486 (0.06)	1483 (0.05)	1465 (0.1)	1469 (0.07)	1413	1420
$\nu_{13}$ $\text{NH}_2$ twist	$\text{CH}_3\text{NH}_2$	1371 (0.001)	1368 (0.0003)	1408 (0.4)	1445 (0.007)	1357	1339
$\nu_8$ $\text{CO}_2$ symmetric stretch	$\text{CO}_2$	1371 (0)	1364 (0.05)	1289 (2.4)	1302 (2.5)	—	—
$\nu_8$ $^{13}\text{CO}_2$ symmetric stretch	$^{13}\text{CO}_2$	1371 (0)	1364 (0.05)	1280 (2.3)	1292 (2.3)	—	—
$\nu_7, \nu_{14}$ $\text{CH}_3$ rocking	$\text{CH}_3\text{NH}_2$	1195 (0.1)	1193 (0.07)	1139 (0.3)	1146 (0.2)	1167, 1146	1156
$\nu_8$ $\text{CN}$ stretching	$\text{CH}_3\text{NH}_2$	1069 (0.1)	1066 (0.1)	1054 (0.1)	1039 (0.4)	1041	1042
$\nu_9$ $\text{NH}_2$ wagging sym (IR inert)	$\text{CH}_3\text{NH}_2$	988 (0)	990 (0)	944 (0.4), 1150 (0.1)	966 (0), 1184 (0)	—	—
$\nu_9$ $\text{NH}_2$ wagging asym (IR act)	$\text{CH}_3\text{NH}_2$	876 (2.8)	895 (2.5)	1371 (2.0)	1413 (1.5)	820	997, 896
$\nu_2$ in plane bending	$\text{CO}_2$	640 (0.5)	647 (0.5)	678 (0.007)	723 (4.1)	667	654
$\nu_2$ out of plane bending	$\text{CO}_2$	640 (0.5)	595 (1.5)	709 (3.8)	765 (2.2)	667	654

<sup>a</sup> For  $\text{CH}_3\text{NH}_2/\text{CO}_2/(\text{H}_2\text{O})_2$  the first column is where the carbon dioxide is parallel to the  $\text{CH}_3\text{-NH}_2$  bond and the second column is where the carbon dioxide is perpendicular to the  $\text{CH}_3\text{-NH}_2$  bond. <sup>b</sup> Experimental values taken from Table 1 in ref. 27. <sup>c</sup> Experimental values taken from Table 1 in ref. 75.

The out-of-plane carbon dioxide frustrated rotation which couples with the N(4) atom in methylamine also produces an intense IR vibration at  $709 \text{ cm}^{-1}$  ( $765 \text{ cm}^{-1}$ ) in the parallel (perpendicular) conformers.

The two waters in the  $\text{CH}_3\text{NH}_2/\text{CO}_2/(\text{H}_2\text{O})_2$  complex also cause significant vibrational shifts involving the N–H vibrations on methylamine. This is partly due to the hydrogen atoms of the amino group forming a hydrogen-bond with a water molecule resulting in the N–H stretching frequency being reduced. The largest N–H frequency changes occur for the symmetric and asymmetric  $\text{NH}_2$  stretch modes and the computed N–H stretch frequencies are now in much closer agreement with the experimentally assigned values given in Table 2 of the Bossa *et al.*<sup>75</sup> paper. In addition, we find a  $495 \text{ cm}^{-1}$  increase in the IR active asymmetric  $\text{NH}_2$  wagging mode at  $1371 \text{ cm}^{-1}$  ( $1413 \text{ cm}^{-1}$ ) in the parallel (perpendicular)  $\text{CH}_3\text{NH}_2/\text{CO}_2/(\text{H}_2\text{O})_2$  conformers.

**$\text{CH}_3\text{NH}_2/\text{CO}_2/(\text{H}_2\text{O})_{0-20}$ .** We find less dramatic changes in vibrational frequencies as the number of water molecules in the  $\text{CH}_3\text{NH}_2/\text{CO}_2/(\text{H}_2\text{O})_n$  complex is increased beyond two. In Fig. 10 and Table 3, we show how the computed vibrational frequencies for carbon dioxide vary as the number of  $\text{H}_2\text{O}$  surrounding the  $\text{CH}_3\text{NH}_2/\text{CO}_2$  complex increases. The largest frequency shifts are found for  $\nu_3$  asymmetric stretching mode of carbon dioxide with the maximum shift occurring as the first two waters are added to the complex. The addition of one  $\text{H}_2\text{O}$  to  $\text{CH}_3\text{NH}_2/\text{CO}_2$  complex only causes a  $13 \text{ cm}^{-1}$  red shift in the computed frequency of the  $\nu_3$  mode. After the large red shift in  $\nu_3$  with 2 waters to  $1989 \text{ cm}^{-1}$ , the addition of more  $\text{H}_2\text{O}$  causes the  $\nu_3$  mode to more slowly to red shift to the lowest computed value at  $1798 \text{ cm}^{-1}$  when  $12\text{H}_2\text{O}$  are present in the cluster. Between 12 and 20 water clusters, the frequency

of the  $\nu_3$  mode only fluctuates slightly and is computed to be at  $1799 \text{ cm}^{-1}$  in the 20 water cluster.

The symmetric  $\nu_8$  stretching mode jumps from  $1364 \text{ cm}^{-1}$  in the complex with zero waters to  $1289 \text{ cm}^{-1}$  ( $1302 \text{ cm}^{-1}$ ) with two waters for parallel (perpendicular) conformers and then slowly varies to  $1292 \text{ cm}^{-1}$  in the  $\text{CH}_3\text{NH}_2/\text{CO}_2/(\text{H}_2\text{O})_8$  cluster. Then as the methyl group of methylamine starts to become coordinated by water molecules the  $\nu_8$  mode blue shifts to eventually arrive back at  $1365 \text{ cm}^{-1}$  in the cluster containing 20 waters. The increase in the  $\nu_8$  stretching frequency is unusual in that it appears to be correlating with an increase, rather than a decrease, in the C–O bond length in carbon dioxide. An important feature of the symmetric  $\nu_8$  mode is that it becomes more IR active with increased carbon dioxide bending. In the presence of one water molecule the  $\nu_8$  IR intensity is computed to be  $0.2 \times 10^{-17} \text{ cm molecule}^{-1}$ , while adding up to 10 waters the  $\nu_8$  IR intensity continues to increase with values of  $2.4 \times 10^{-17}$ ,  $4.4 \times 10^{-17}$  and  $5.5 \times 10^{-17} \text{ cm molecule}^{-1}$  for  $\text{CH}_3\text{NH}_2/\text{CO}_2/(\text{H}_2\text{O})_n$  where  $n = 2, 6,$  and  $10$ , respectively. Between 12 and 20 waters, the  $\nu_8$  IR intensity decreases slightly to  $3.7 \times 10^{-17} \text{ cm molecule}^{-1}$  in the  $\text{CH}_3\text{NH}_2/\text{CO}_2/(\text{H}_2\text{O})_{20}$  cluster. The IR intensity of the  $\nu_8$  symmetric mode increases with larger differences in the C(1)–O(2) and C(1)–O(3) distances. For example, in all the clusters where the  $\text{CO}_2$  is bent, the  $n = 20$  cluster has one of the smallest  $\nu_8$  IR intensity and the smallest difference between the 2 CO bond distances.

Table 3 and Fig. 10 show that the carbon dioxide bending mode frequency shifts from  $647 \text{ cm}^{-1}$  with zero waters to  $795 \text{ cm}^{-1}$  on adding up to 20 water molecules to the  $\text{CH}_3\text{NH}_2/\text{CO}_2$  cluster. Whereas, the carbon dioxide frustrated rotation frequency ranges from  $595 \text{ cm}^{-1}$  to  $867 \text{ cm}^{-1}$  with 0 to 20 waters in the cluster and becomes increasingly mixed with the methylamine

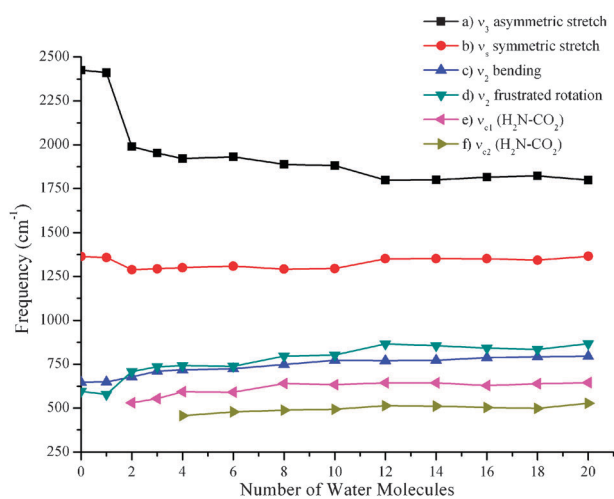


**Fig. 10** Variation of the carbon dioxide vibrational frequencies: (a) asymmetric stretch, (b) symmetric stretch, (c) bending, (d) frustrated rotation; and the N–C stretching frequencies: (e) and (f) which arise from  $\text{H}_2\text{N}-\text{CO}_2$  coupling when there are at least two water clusters.

vibrational modes as the carbon dioxide interacts more strongly with methylamine. As a consequence of this interaction, the calculations revealed two new N–C stretching modes, one is present when there at least two waters and another one occurs with four waters in the cluster (Fig. 10e and f). Both vibrations shift increasingly, from  $530\text{ cm}^{-1}$  to  $645\text{ cm}^{-1}$  (from 2 to 20 water clusters) and  $456\text{ cm}^{-1}$  to  $527\text{ cm}^{-1}$  (from 4 to 20 water clusters) and are IR active with the

intensities of  $0.8 \times 10^{-17}$ ,  $0.3 \times 10^{-17}$ ,  $0.3 \times 10^{-17}$  and  $1.1 \times 10^{-17}\text{ cm molecule}^{-1}$ , respectively.

**CW results.** The carbon dioxide stretching and bending vibrational frequencies computed for the crystalline water clusters CWI, CWII and CWIII are also given in Table 3. As more water is added to CWI to eventually produce the CWIII cluster we find changes in the carbon dioxide vibrational frequencies which parallel the trends found in the frequency calculations on the  $\text{CH}_3\text{NH}_2/\text{CO}_2/(\text{H}_2\text{O})_n$  clusters with amorphous water. Consistent with the geometry results in the previous subsections, the CWI carbon dioxide vibration frequencies resemble the amorphous water cluster with 2 water molecules, CWII has vibrational frequencies similar to those when  $n = 8$ , and the CWIII results resemble the  $n = 16$  cluster. In all of the ice structures, we also found out that the carbon dioxide frustrated rotation couples with the N–C stretching mode.

**Comparison with experimental IR spectra.** Experimentally, a  $\text{COO}^-$  group in a salt or zwitterion is typically characterized by two strong IR bands with frequencies in the range  $1550$  to  $1625\text{ cm}^{-1}$  and  $1400$  to  $1450\text{ cm}^{-1}$ , where the bands correspond to the asymmetric and symmetric C–O stretch modes, respectively.<sup>27,30,75,77,78</sup> Included in Table 3 are the experimental frequencies assigned to these two modes taken from Table 1 of the Bossa *et al.* paper for the pure methylcarbamate ( $\text{CH}_3\text{NHCO}_2^-$ ) and glycinate ( $\text{NH}_2\text{CH}_2\text{CO}_2^-$ ) anions with a methylammonium ( $\text{CH}_3\text{NH}_3^+$ ) counter cation.<sup>30</sup> We also included in Table 3 the IR frequencies used by Holtom *et al.* (Table 4) to characterize the glycine zwitterion formed in a

**Table 3** The N(4)–C(1) distance (in Å) and the carbon dioxide bond angle (in °) in the methylamine–carbon dioxide complex and the computed IR absorption frequencies ( $\text{cm}^{-1}$ ) for the bending  $\nu_2$ , symmetric stretch  $\nu_s$ , and asymmetric stretch  $\nu_3$  vibrational modes for carbon dioxide. The IR intensities ( $\times 10^{-17}\text{ cm molecule}^{-1}$ ) are given in parentheses. The experimental vibrational frequencies are included for comparison at the bottom of the table

Number of water	N(4)–C(1)	O(2)–C(1)–O(3)	$\nu_2$ in plane bending	$\nu_s$ symmetric stretch	$\nu_3$ asymmetric stretch
0	2.808	175.1	647 (0.5)	1364 (0.05)	2424 (8.4)
1	2.691	172.1	648 (0.5)	1358 (0.2)	2411 (9.4)
2	1.700	140.1	678 (0.07)	1289 (2.4)	1989 (8.9)
3	1.646	137.8	710 (0.9)	1294 (3.1)	1953 (9.3)
4	1.602	135.8	718 (0.3)	1300 (4.1)	1921 (8.9)
6	1.604	135.8	725 (0.7)	1309 (4.4)	1931 (9.0)
8	1.555	133.0	748 (2.9)	1292 (5.4)	1888 (11.0)
10	1.548	132.7	772 (2.3)	1295 (5.5)	1881 (11.0)
12	1.513	130.6	770 (1.0)	1351 (4.8)	1798 (8.2)
14	1.515	130.6	773 (0.9)	1352 (4.4)	1800 (8.7)
16	1.528	131.4	788 (8.0)	1351 (4.1)	1815 (9.0)
18	1.539	132.2	793 (6.7)	1343 (3.8)	1823 (7.3)
20	1.512	130.0	795 (1.4)	1365 (3.7)	1799 (11.0)
CWI	1.707	141.0	676 (1.0)	1307 (3.5)	1992 (9.5)
CWII	1.554	133.1	763 (1.2)	1336 (4.0)	1873 (10.0)
CWIII	1.523	131.1	770 (0.1)	1351 (4.8)	1825 (10.0)
$\text{CO}_2^-$	—	133.7	732 (0.2)	1343 (0.2)	1705 (8.0)
$\text{CH}_3\text{NHCO}_2^-$	1.477	131.0	892 (1.9)	1321 (4.4)	1787 (7.2)
$\text{NH}_2\text{CH}_2\text{CO}_2^-$	—	129.8	569 (0.09)	1378 (3.4)	1750 (5.9)
Experimental frequencies					
$\text{CH}_3\text{NHCO}_2^-$ <sup>a</sup>				1410	1578
$\text{NH}_2\text{CH}_2\text{CO}_2^-$ <sup>a</sup>				1403	1565
$\text{NH}_3^+\text{CH}_2\text{CO}_2^-$ <sup>b</sup>				1413, 1401	1596

<sup>a</sup> Experimental values taken from Table 1 in ref. 30. <sup>b</sup> Experimental values taken from Table 4 in ref. 27.

$\text{CH}_3\text{NH}_2/\text{CO}_2$  ice at 10 K.<sup>27</sup> The Bossa *et al.* frequency data show that it will be difficult to use IR spectroscopy to unambiguously distinguish between the methylcarbamate and glycinate anions.<sup>30</sup> The Holtom *et al.*<sup>27</sup> frequencies assigned to the glycine zwitterion are also in the same region as the Bossa *et al.*<sup>30</sup> assignments. The slightly higher asymmetric stretch frequency obtained by Holtom *et al.*<sup>27</sup> could be consistent with forming the glycine zwitterion  $\text{NH}_3^+\text{CH}_2\text{CO}_2^-$ . We included in Table 3 the computed  $\text{CO}_2^-$  vibrational frequencies for the anions  $\text{CO}_2^-$ ,  $\text{CH}_3\text{NHCO}_2^-$  and  $\text{NH}_2\text{CH}_2\text{CO}_2^-$ . These calculations show that  $\text{CO}_2^-$  on its own does not have a very intense symmetric stretching mode. Secondly, although these  $\text{CO}_2^-$  computed frequencies are not in quantitative agreement with the experimental frequencies, they do show trends similar to those found experimentally by Bossa *et al.*<sup>30</sup> and Holtom *et al.*<sup>27</sup> More specifically, the  $\text{CO}_2^-$  calculations overestimate the  $\text{CO}_2$  asymmetric stretch by  $\sim 200\text{ cm}^{-1}$  and underestimate the  $\text{CO}_2$  symmetric stretch by  $\sim 80\text{ cm}^{-1}$ .

Our geometry optimization results in this paper suggest that the methylcarbamic acid zwitterion is formed when two or more water molecules are associated with the  $\text{CH}_3\text{NH}_2/\text{CO}_2$  complex. Comparison of  $\text{CO}_2$  symmetric stretch frequency and intensity for the different  $\text{CH}_3\text{NH}_2/\text{CO}_2/(\text{H}_2\text{O})_n$  clusters in Table 3 with the values computed for  $\text{CH}_3\text{NHCO}_2^-$  and  $\text{NH}_2\text{CH}_2\text{CO}_2^-$  indicates that the symmetric stretch frequency calculations are consistent with the Bossa *et al.* and Holtom *et al.* experimental results. However, the results in Table 3 suggest asymmetric  $\text{CO}_2$  stretching frequency for the  $\text{CH}_3\text{NH}_2^+\text{CO}_2^-$  zwitterion in  $\text{CH}_3\text{NH}_2/\text{CO}_2/(\text{H}_2\text{O})_n$  will be shifted to a slightly higher frequency relative to that for the  $\text{CH}_3\text{NHCO}_2^-$  and  $\text{NH}_2\text{CH}_2\text{CO}_2^-$  anions. Unfortunately, our calculations also suggest this shift may be difficult to observe experimentally because, even though the intensity of the  $\text{CO}_2$  asymmetric stretch vibration is strong, it will be lost in the IR band produced by the many water bending vibrations.

For example, Bossa *et al.* have measured the IR spectra of a  $\text{H}_2\text{O} : \text{CO}_2 : \text{CH}_3\text{NH}_2$  with component ratio 10 : 3 : 0.5 at 10 K.<sup>30</sup> If each methylamine molecule produced one methylcarbamic acid zwitterion, the experimental situation would approximately match the  $\text{CH}_3\text{NH}_2/\text{CO}_2/(\text{H}_2\text{O})_{20}$  cluster and in our calculations on this cluster we found the intensity of the  $\text{CO}_2$  asymmetric stretch is much smaller than the intensity of the band arising from the 20 water bending modes. The IR spectra shown in Fig. 1a of the Bossa *et al.*<sup>30</sup> paper do show an interesting shoulder at  $1600\text{ cm}^{-1}$  on the water bending peak. Bossa *et al.* assign this shoulder to a  $\text{NH}_2$  scissor vibration. However, our frequency calculations on the different  $\text{CH}_3\text{NH}_2/\text{CO}_2/(\text{H}_2\text{O})_n$  clusters find the intensity for the  $\text{NH}_2$  scissor vibration to be low as well as being lower than the intensity for the asymmetric stretch for bent  $\text{CO}_2^-$ . After the initial  $\text{H}_2\text{O} : \text{CO}_2 : \text{CH}_3\text{NH}_2$  ice deposition at 10 K, Bossa *et al.* raised the ice temperature to cause the eventual desorption of all the water at 200 K. Since our calculations indicate the  $\text{CH}_3\text{NH}_2^+\text{CO}_2^-$  zwitterion to be only stable when there is water present, we would not expect Bossa *et al.* to find any evidence for the methylcarbamic acid zwitterion in their experiments. Our calculations imply there might be a greater chance of finding an asymmetric  $\text{CO}_2$  stretching vibration

confirming formation of the methylcarbamic acid zwitterion, at a higher frequency than the  $1565\text{ cm}^{-1}$  observed for the methylcarbamate ion, in an ice such as  $\text{H}_2\text{O} : \text{CO}_2 : \text{CH}_3\text{NH}_2 = 4 : 1 : 1$ , where there is less water.

#### 4. Conclusions

Although the detection of the simplest amino acid, glycine, in the ISM has not been confirmed yet, its detection in meteorites and cometary samples motivated this study since it can have the interstellar origin. Possible interactions between methylamine and carbon dioxide within water ice mantles in the ISM were investigated by simulating the conditions in amorphous and crystalline water ice environments with DFT calculations in order to understand the formation of glycine and its isomer methylcarbamic acid. In both of the amorphous and crystalline water ice environments, carbon dioxide favored to be close to the amino end of the methylamine rather than the methyl end, and surrounding water molecules formed hydrogen bond bridges between methylamine and carbon dioxide. These bridges play an important role in the interaction of methylamine and carbon dioxide, drawing carbon dioxide toward the amino group of methylamine, ending up with a stronger interaction, shortened N–C bond length and causing carbon dioxide to be significantly bent. In our calculations, although we did not detect a hydrogen atom transfer from methylamine or surrounding water molecules to carbon dioxide, we found a considerable charge transfer from methylamine to carbon dioxide suggesting the formation of the  $\text{CH}_3\text{NH}_2^+\text{CO}_2^-$  zwitterionic complex in the presence of two or more water molecules. Additionally, increasing trend in dipole moments also supports this suggestion.

Vibrational frequency calculations show that isolated carbon dioxide and methylamine fundamentals agreed well with the experimental<sup>75,76</sup> IR frequency assignments. Only small shifts ( $<20\text{ cm}^{-1}$ ) are observed in the vibrational frequencies of the  $\text{CH}_3\text{NH}_2/\text{CO}_2$  van der Waals complex from the isolated methylamine and carbon dioxide due to the weak interaction in between them. On the other hand, this interaction caused originally IR inactive carbon dioxide symmetric stretching to become weakly IR active (intensity  $0.05 \times 10^{-17}\text{ cm molecule}^{-1}$ ), and also carbon dioxide bending mode to split into the separate in-plane ( $647\text{ cm}^{-1}$ ) and out-of-plane ( $595\text{ cm}^{-1}$ ) vibration modes. By the addition of two water molecules, asymmetric stretch of carbon dioxide is *drastically red shifted* by  $435\text{ cm}^{-1}$  to  $1989\text{ cm}^{-1}$ , and the intensity of carbon dioxide symmetric stretch became strongly IR active ( $2.4 \times 10^{-17}\text{ cm molecule}^{-1}$ ) as a result of relatively strong interaction between methylamine and carbon dioxide with the help of water bridges. In addition to the changes in the carbon dioxide vibrations, the frequencies of N–H vibrations, asymmetric/symmetric stretch and wagging modes of the amino group are also shifted when hydrogen bonds are formed between the hydrogen atoms of the amino group and water molecules. Our vibrational frequency results obtained from both amorphous and crystalline water ice calculations at low temperature suggest that the  $\text{CH}_3\text{NH}_2/\text{CO}_2/(\text{H}_2\text{O})_2$  complex can be considered as a prototype complex to simulate the interactions between methylamine and carbon dioxide in

the ISM, since slight changes in vibrational frequencies are observed as the number of water molecules surrounding methylamine and carbon dioxide is increased beyond two. Our results for the shifts in the vibrational frequencies and the changes in the vibration intensities suggest that these parameters can be used as tracers or diagnostic tools in the investigation of methylamine carbon dioxide interactions within water ice mantels.

In summary, our investigations suggest that the methylcarbamic acid zwitterion,  $\text{CH}_3\text{NH}_2^+\text{CO}_2^-$ , can be produced in water dominated ice from the interaction of methylamine and carbon dioxide. This zwitterion can be regarded as a precursor or pre-biotic source of the simple amino acids in ISM and can also act as a reservoir for carbon dioxide and methylamine. On the other hand, further studies are necessary to investigate the photochemical behavior of  $\text{CH}_3\text{NH}_2^+\text{CO}_2^-$  because no spontaneous hydrogen transfer to form a neutral acid, such as methylcarbamic acid  $\text{CH}_3\text{NHCOOH}$ , is observed in our calculations.

## Acknowledgements

This project was supported by the W.M. Keck Foundation and the NASA Astrobiology Institute under Cooperative Agreement no. NNA09DA77A issued through the Office of Space Science. The authors are also grateful for the computing assistance from Mr. M. Belcaid and the generous computing resources provided by the Dell Cluster at the University of Hawaii.

## References

- J. M. Hollis, F. J. Lovas and P. R. Jewell, *Astrophys. J.*, 2000, **540**, L107–L110.
- D. J. Hollenbach and H. A. Thronson, *Interstellar Processes*, Reidel, Dordrecht, 1987.
- A. G. G. M. Tielens and L. J. Allamandola, in *Interstellar Processes*, ed. D. J. Hollenbach and H. A. Thronson, Reidel, Dordrecht, 1987, pp. 397–469.
- Carbon in the Galaxy: Studies from Earth and Space*, Report NASA-SP-3061, NASA, Washington, D.C., 1990.
- Interstellar Dust*, Report NASA-SP-3036, NASA, Washington, D.C., 1989.
- J. Oro, *Nature*, 1961, **190**, 389–390.
- A. Brack, *Adv. Space Res.*, 1999, **24**, 417–433.
- U. Meierhenrich, W. H. P. Thiemann and H. Rosenbauer, *Chirality*, 1999, **11**, 575–582.
- D. E. Newton, *Chemistry of Space*, Facts on File Inc., New York, 2007.
- J. R. Cronin and S. Pizzarello, *Science*, 1997, **275**, 951–955.
- J. R. Cronin and S. Pizzarello, *Adv. Space Res.*, 1999, **23**, 293–299.
- P. Ehrenfreund, D. P. Glavin, O. Botta, G. Cooper and J. L. Bada, *Proc. Natl. Acad. Sci. U. S. A.*, 2001, **98**, 2138–2141.
- M. H. Engel and S. A. Macko, *Precambrian Res.*, 2001, **106**, 35–45.
- K. A. Kvenvolden, J. Lawless, K. Pering, E. Peterson, J. Flores, C. Ponnampuruma, I. R. Kaplan and C. Moore, *Nature*, 1970, **228**, 923–926.
- J. R. Cronin, G. W. Cooper and S. Pizzarello, *Adv. Space Res.*, 1994, **15**, 91–97.
- S. A. Sandford, J. Aleon, C. M. O. D. Alexander, T. Araki, S. Bajt, G. A. Baratta, J. Borg, J. P. Bradley, D. E. Brownlee, J. R. Brucato, M. J. Burchell, H. Busemann, A. Butterworth, S. J. Clemett, G. Cody, L. Colangeli, G. Cooper, L. D'Hendecourt, Z. Djouadi, J. P. Dworkin, G. Ferrini, H. Fleckenstein, G. J. Flynn, I. A. Franchi, M. Fries, M. K. Gilles, D. P. Glavin, M. Gounelle, F. Grossemy, C. Jacobsen, L. P. Keller, A. L. D. Kilcoyne, J. Leitner, G. Matrajt, A. Meibom, V. Mennella, S. Mostefaoui, L. R. Nittler, M. E. Palumbo, D. A. Papanastassiou, F. Robert, A. Rotundi, C. J. Snead, M. K. Spencer, F. J. Stadermann, A. Steele, T. Stephan, P. Tsou, T. Tyliczszak, A. J. Westphal, S. Wirrick, B. Wopenka, H. Yabuta, R. N. Zare and M. E. Zolensky, *Science*, 2006, **314**, 1720–1724.
- D. P. Glavin, J. P. Dworkin and S. A. Sandford, *Meteorit. Planet. Sci.*, 2008, **43**, 399–413.
- Y.-J. Kuan, S. B. Charnley, H.-C. Huang, W.-L. Tseng and Z. Kisiel, *Astrophys. J.*, 2003, **593**, 848–867.
- L. E. Snyder, F. J. Lovas, J. M. Hollis, D. N. Friedel, P. R. Jewell, A. Remijan, V. V. Ilyushin, E. A. Alekseev and S. F. Dyubko, *Astrophys. J.*, 2005, **619**, 914–930.
- P. A. Jones, M. R. Cunningham, P. D. Godfrey and D. M. Cragg, *Mon. Not. R. Astron. Soc.*, 2007, **374**, 579–589.
- M. R. Cunningham, P. A. Jones, P. D. Godfrey, D. M. Cragg, I. Bains, M. G. Burton, P. Calisse, N. H. M. Crighton, S. J. Curran, T. M. Davis, J. T. Dempsey, B. Fulton, M. G. Hidas, T. Hill, L. Kedziora-Chudczer, V. Minier, M. B. Pracy, C. Purcell, J. Shobbrook and T. Travouillon, *Mon. Not. R. Astron. Soc.*, 2007, **376**, 1201–1210.
- K. Kobayashi, H. Masuda, K.-I. Ushio, A. Ohashi, H. Yamanashi, T. Kaneko, J.-I. Takahashi, T. Hosokawa, H. Hashimoto and T. Saito, *Adv. Space Res.*, 2001, **27**, 207–215.
- V. Blagojevic, S. Petrie and D. K. Bohme, *Mon. Not. R. Astron. Soc.*, 2003, **339**, L7–L11.
- K. Kobayashi, T. Kasamatsu, T. Kaneko, J. Koike, T. Oshima, T. Saito, T. Yamamoto and H. Yanagawa, *Adv. Space Res.*, 1995, **16**, 21–26.
- G. M. Munoz Caro, U. J. Meierhenrich, W. A. Schutte, B. Barbler, A. A. Segovia, H. Rosenbauer, W. H. P. Thiemann, A. Brack and J. M. Greenberg, *Nature*, 2002, **416**, 403–406.
- M. P. Bernstein, J. P. Dworkin, S. A. Sandford, G. W. Cooper and L. J. Allamandola, *Nature*, 2002, **416**, 401–403.
- P. D. Holtom, C. J. Bennett, Y. Osamura, N. J. Mason and R. I. Kaiser, *Astrophys. J.*, 2005, **626**, 940–952.
- C.-W. Lee, J.-K. Kim, E.-S. Moon, Y. C. Minh and H. Kang, *Astrophys. J.*, 2009, **697**, 428–435.
- J.-B. Bossa, F. Borget, F. Duvernay, P. Theule and T. Chiavassa, *J. Phys. Org. Chem.*, 2010, **23**, 333–339.
- J. B. Bossa, F. Duvernay, P. Theule, P. Borget, L. d'Hendecourt and T. Chiavassa, *Astron. Astrophys.*, 2009, **506**, 601–608.
- N. Goldman, E. J. Reed, L. E. Fried, I. F. William Kuo and A. Maiti, *Nat. Chem.*, 2010, **2**, 949–954.
- A. G. Csaszar, *J. Am. Chem. Soc.*, 1992, **114**, 9568–9575.
- P. D. Godfrey and R. D. Brown, *J. Am. Chem. Soc.*, 1995, **117**, 2019–2023.
- O. Bludsky, J. Chocholousova, J. Vacek, F. Huisken and P. Hobza, *J. Chem. Phys.*, 2000, **113**, 4629–4635.
- L. F. Pacios and P. C. Gomez, *J. Mol. Struct. (THEOCHEM)*, 2001, **544**, 237–251.
- S. Maeda and K. Ohno, *Chem. Phys. Lett.*, 2004, **398**, 240–244.
- J. H. Jensen and M. S. Gordon, *J. Am. Chem. Soc.*, 1995, **117**, 8159–8170.
- A. Chaudhari and S.-L. Lee, *Chem. Phys.*, 2005, **310**, 281–285.
- P. K. Sahu and S.-L. Lee, *J. Mol. Model.*, 2008, **14**, 385–392.
- S. M. Bachrach, *J. Phys. Chem. A*, 2008, **112**, 3722–3730.
- C. Espinoza, J. Szczepanski, M. Vala and N. C. Polfer, *J. Phys. Chem. A*, 2010, **114**, 5919–5927.
- J. Andres, V. Moliner, J. Krechl and E. Silla, *Int. J. Quantum Chem.*, 1993, **45**, 433–444.
- M. H. Jamroz, J. C. Dobrowolski and M. A. Borowiak, *J. Mol. Struct.*, 1997, **404**, 105–111.
- A. Khan, *J. Mol. Struct. (THEOCHEM)*, 2003, **664–665**, 237–245.
- N. R. Jena and P. C. Mishra, *Theor. Chem. Acc.*, 2005, **114**, 189–199.
- K. I. Peterson, R. D. Suenram and F. J. Lovas, *J. Chem. Phys.*, 1991, **94**, 106–117.
- A. J. Leadbetter, R. C. Ward, J. W. Clark, P. A. Tucker, T. Matsuo and H. Suga, *J. Chem. Phys.*, 1985, **82**, 424–428.
- <http://avogadro.openmolecules.net>.
- M. W. Schmidt, K. K. Baldrige, J. A. Boatz, S. T. Elbert, M. S. Gordon, J. H. Jensen, S. Koseki, N. Matsunaga, K. A. Nguyen, S. Su, T. L. Windus, M. Dupuis and J. A. Montgomery, *J. Comput. Chem.*, 1993, **14**, 1347–1363.
- A. D. Becke, *Phys. Rev. A*, 1988, **38**, 3098–3100.

- 
- 51 C. Lee, W. Yang and R. G. Parr, *Phys. Rev. B: Condens. Matter Mater. Phys.*, 1988, **37**, 785–789.
- 52 A. D. Becke, *J. Chem. Phys.*, 1993, **98**, 5648–5652.
- 53 P. C. Hariharan and J. A. Pople, *Theor. Chim. Acta*, 1973, **28**, 213–222.
- 54 R. Krishnan, J. S. Binkley, R. Seeger and J. A. Pople, *J. Chem. Phys.*, 1980, **72**, 650–654.
- 55 M. J. Frisch, J. A. Pople and J. S. Binkley, *J. Chem. Phys.*, 1984, **80**, 3265–3269.
- 56 P. N. Day, J. H. Jensen, M. S. Gordon, S. P. Webb, W. J. Stevens, M. Krauss, D. Garmer, H. Basch and D. Cohen, *J. Chem. Phys.*, 1996, **105**, 1968–1986.
- 57 G. N. Merrill and M. S. Gordon, *J. Phys. Chem. A*, 1998, **102**, 2650–2657.
- 58 P. N. Day, R. Pachter, M. S. Gordon and G. N. Merrill, *J. Chem. Phys.*, 2000, **112**, 2063–2073.
- 59 I. Adamovic, M. A. Freitag and M. S. Gordon, *J. Chem. Phys.*, 2003, **118**, 6725–6732.
- 60 M. S. Gordon, M. A. Freitag, P. Bandyopadhyay, J. H. Jensen, V. Kairys and W. J. Stevens, *J. Phys. Chem. A*, 2001, **105**, 293–307.
- 61 H. Li, H. M. Netzloff and M. S. Gordon, *J. Chem. Phys.*, 2006, **125**, 194103.
- 62 W. Chen and M. S. Gordon, *J. Chem. Phys.*, 1996, **105**, 11081–11090.
- 63 A. Bondi, *J. Phys. Chem.*, 1964, **68**, 441–451.
- 64 J. Pipek and P. G. Mezey, *J. Chem. Phys.*, 1989, **90**, 4916–4926.
- 65 F. Tordini, A. Bencini, M. Bruschi, L. De Gioia, G. Zampella and P. Fantucci, *J. Phys. Chem. A*, 2003, **107**, 1188–1196.
- 66 M. H. Jamroz, J. C. Dobrowolski and M. A. Borowiak, *Vib. Spectrosc.*, 2000, **22**, 157–161.
- 67 S.-W. Park, S. Im, S. Lee and C. Desfrancois, *Int. J. Quantum Chem.*, 2007, **107**, 1316–1327.
- 68 P. Jenniskens and D. F. Blake, *Astrophys. J.*, 1996, **473**, 1104–1113.
- 69 H.-B. Xie, C.-B. Shao and Y.-H. Ding, *Astrophys. J.*, 2007, **670**, 449–456.
- 70 H. M. Cuppen and E. Herbst, *Astrophys. J.*, 2007, **668**, 294–309.
- 71 M. E. Palumbo, *J. Phys.: Conf. Ser.*, 2005, **6**, 211–216.
- 72 L. Hornekaer, A. Baurichter, V. V. Petrunin, A. C. Luntz, B. D. Kay and A. Al-Halabi, *J. Chem. Phys.*, 2005, **122**, 124701.
- 73 A. Rimola, M. Sodupe and P. Ugliengo, *Phys. Chem. Chem. Phys.*, 2010, **12**, 5285–5294.
- 74 A. Allouche, P. Verlaque and J. Pourcin, *J. Phys. Chem. B*, 1998, **102**, 89–98.
- 75 J.-B. Bossa, F. Borget, F. Duvernay, P. Theule and T. Chiavassa, *J. Phys. Chem. A*, 2008, **112**, 5113–5120.
- 76 R. D. Johnson, NIST Computational Chemistry Comparison and Benchmark Database (CCCBDB), [www.cccbdb.nist.gov](http://www.cccbdb.nist.gov), 2010.
- 77 M. E. Jacox and W. E. Thompson, *J. Chem. Phys.*, 1989, **91**, 1410–1416.
- 78 M. T. Rosado, M. L. T. S. Duarte and R. Fausto, *Vib. Spectrosc.*, 1998, **16**, 35–54.